
ADDIS ABABA UNIVERSITY

INSTITUTE OF TECHNOLOGY

SCHOOL OF CIVIL AND ENVIRONMENTAL ENGINEERING

# GIS-BASED MODELING FOR FOREST FIRE EXTENT MAPPING IN SIMEN MOUNTAINS NATIONAL PARK, ETHIOPIA

A thesis submitted to School of Civil and Environmental Engineering Graduate Studies of Addis Ababa Institute of Technology in Partial Fulfillment of the Requirement for the Degree Masters of Science in Geodesy and Geomatics (specialization in Geomatics)

BY: SHUMET MENGESHA

ADVISOR: WORKU ZEWDIE (PhD)

March / 2022

ADDIS ABABA

**APPROVAL SHEET**

This undersigned hear by certify that they have read and recommend to Addis Ababa university institute of technology school of civil and environmental engineering for acceptance a thesis entitled: "GIS-based modeling for forest fire extent mapping in Simen Mountains National Park, Ethiopia" By Shumet Mengesha In partial fulfillment of the Requirement for the Degree Masters of Science in Geodesy and Geomatics (specialization in Geomatics).

**Approved By the Board of Examiners:**

| | | |
|---|---|---|
| Dr. Kotiku Zewdie<br>Advisor | Signature | 03/05/2022<br>Date |
| Dr. Sisay Walelign<br>Internal Examiner | Signature | 24-05/2022<br>Date |
| Dr. K. V. SURYABHAGAVAN<br>External Examiner | Signature | 14. 04. 2022<br>Date |
| Dr. Mebruk Mohammed (Dr.-Ing.)<br>Dean, Faculty of Civil & Environmental Engineering<br>Chairman | Signature | Date |



I

**DECLARATION**

I hereby declare that the thesis entitled "GIS-based modeling for forest fire extent mapping in Simen Mountains National Park, Ethiopia" has been, carried out by me under the supervision of Dr.Worku Zewdie. School of Civil and Environmental Engineering, Addis Ababa University during the year 2020-2021 as a part of Master of Science in Geodesy and Geomatics (Specialization in Geomatics). I further declare that this work has not been, submitted to any other University or Institution for the award of any Degree or Diploma.

| | | |
|---|---|---|
| Author Name | Signature | Date |
| Advisor | Signature | Date |

## Acknowledgements

First and foremost, I want to express my gratitude to the almighty God and His Mother, the Blessed Virgin Mary, for providing me with the strength and health necessary to complete my study.

Second, I would like to express special thanks to my advisor, D/r Worku Zewdie, from the Remote Sensing Research and Development Department of Ethiopian Space Science, for his immeasurable and priceless support, constructive comments, and devoting precious time to reading, guiding, and correcting this research. Without him, this paper would not be in its present form. I pray that God blesses you and your family.

Now it is time to thank Mr. Natnael Agegnehu, who is an unreplaceable person for me. Words can't express his efforts to help me not only contribute to this paper but also in all my life. He is a man who upgraded me in different ways. I wish him success in his life all the time. In addition, I would like to thank teachers Dr. Andinet Ashagrie, Dr. Birhan Gesesse and others for providing me with the fundamental knowledge I needed to complete my thesis. I wish peace and health as well as success in your life.

Finally, I would like to express my thanks to all my family, especially my mother, Yalemtsehay Tsega, and my father, Mengesha Getahun, who have supported and encouraged me throughout my life to be an improved and effective person. I also would like to express my genuine thanks to my wife, Amarech Fentahun, for her kindness and tolerance while doing my thesis work.

# Contents

# List of Figures

# List of Tables

# List of Acronyms

| | |
|---|---|
| ArcGIS | Aeronautical Reconnaissance Coverage Geographic Information System |
| DEM | Digital Elevation Model |
| dNBR | Difference Normalized Burn Ratio |
| ETM+ | Enhanced Thematic Mapper plus |
| ERDAS | Earth Resource Data Analysis System |
| EWCA | Ethiopian Wildlife Conservation Authority |
| FAO | Food And Agricultural Organization |
| GIS | Geographic Information System |
| KML | Keyhole Markup Language |
| LULC | Land Use and Land Cover |
| MASL | Meter Above Sea Level |
| MCE | Multi Criteria Evaluation |
| MOA | Ministry Of Agriculture |
| NASA | National Aeronautics and Space Administration |
| NBR | Normalized Burn Ratio |
| NIR | Near Infrared |
| OLI | Operational Land Imagery |
| RS | Remote Sensing |
| SMNP | Simen Mountains National Park |
| SRTM | Shuttle Radar Topography Mission |
| SWIR | Short wave infrared |
| TIFF | Tagged Image File Format |
| TIRS | Thermal Infrared Sensor |
| UNESCO | United Nations Educational, Scientific and Cultural Organization |
| USGS | United States Geological Survey |

## Abstract

In recent years, Simen Mountains National Park (SMNP) has been suffering from frequent forest fires. This forest fire has become a significant factor in environmental degradation, destroying forest cover, leading to loss of biodiversity and exposing the underlying soil to erosion and nitrate leaching from agricultural lands. The main aim of this study is to detect and map forest fire extents, assess land use /land cover changes, map fire risk and forecast forest fire in SMNP. Satellite imagery was vital to monitor and map the earlier fire extents of the study area. Accordingly, the biophysical and ignition risk were adopted to analyze the fires occurring in the park. The biophysical risk model utilized four factors that include land use and land cover (LULC), elevation, slope and aspect. LULC was generated from Landsat 7 and 8 of 2010, 2015 and 2019 respectively. Elevation, aspect and slope were calculated from a digital elevation model. These factors are given different weights by using the pairwise comparison method. The ignition sub model was developed using the proximity analysis method, distance from settlements and roads. By integrating, the biophysical risk submodel, ignition risk submodel and the Difference normalized burn ratio (dNBR) index map, the final forest fire risk model was developed. Weighted overlay analysis techniques were used to develop the final forest fire risk model. In all developed models, the degree of fire risk is categorized under very high, high, moderate and low risk. The final forest fire model showed that 67.86km$^2$ (16.47%), 78.53km$^2$ (19.06%), 191.82km$^2$ (46.56%) and 73.79km$^2$ (17.91%) area of SMNP are categorized under very high, high, moderate and low risk, respectively. Therefore the result shows that there is a significant area under fire risk, which needs frequent follow up.



**Keywords:** Fire severity; biophysical; ignition, Land Use Land Cover; Normalized Burn Ratio

# CHAPTER ONE

# 1. Introduction

## 1.1. Background of the study

Forest is a major natural resource that helps to keep ecological balances (Shiferaw & Suryabhagavan, 2019). Forest is one of the most essential types of resources that humans and other animals rely on, it helps to regulate environmental and biological change by ensuring that soil, water, climate, and rainfall are all in excellent working order and can be sustained (Mideksa, 2009).

According to (Gashaw, 2001) from an economic and ecological point of view, fire offers both advantages and disadvantages. In addition to heating and cooking, it was employed to improve grazing, to remove vegetation in order to facilitate travel, to clear land for agriculture. The seeds of many species remain latent in the soil until the area is burned. Shrubs in dry areas, for example, Acacia, produce vast quantities of hard-coated seeds that germinate only after being heated (Teketay, 2000). Fire, on the other hand, is a major driver of environmental degradation, since it destroys forest cover, resulting in biodiversity loss, as well as exposing the underlying soil to erosion and nitrate escape from agricultural regions (Burgess, 2011). Forest fires that may be controlled or uncontrolled have affected the physical environment, including land cover, land use, biodiversity, climate and the forest ecosystem (Tekalign & Kebede, 2016).

Forest fire frequency is increasing globally. Wildfires have major environmental and ecological issues; threaten human lives, causing massive losses of lives and properties(Parajuli et al., 2020). Wildfires contribute considerably to environmental deterioration, especially global warming, on a worldwide scale (Tan et al., 2007). Forest fires are also a major source of damage to forest resources, and they occur regularly in varying degrees of severity (Ghorbanzadeh et al., 2019). Fire plays an important role in decreasing both the quality and quantity of forest resources. Between 1990 and 2000, Africa lost about 52 million ha of forest, accounting for about 56% of the global reduction in forest cover. Southern Africa (including Tanzania) accounted for about 31% of the forest loss on the continent (Saklani, 2008).

Forest fires in Ethiopia have caused major economic and biological devastation; in early 1984, there were forest fires that affected a large portion of the country's forest area. As a result, a total of 308,198 hectares of forest have been damaged by fire (MOA, 2010). The biggest documented forest fire incidence occurred in the year 2000. In this period, 120 severe forest fires were reported from various parts of the country, and the second largest recorded forest fire incidence occurred in 1993, when 20 events were reported (Tafesse, 2016).

According to the National Forest Service records (State Forest Directorate 1998), fires are caused by human activity and natural events such as lightning. Intentional and unintentional fires are the two most common types of human-caused fires. Unintentional fires are mostly caused by hunters or picnickers' negligence, but intentional fires are mostly related to forest or shrub elimination, land transformation for agricultural objectives, or pasture generation. The majority of wild land fires are caused by a combination of climate and human activities. The forest fire caused significant damage and spread due to the steep topography, high summer temperatures aggravated by high wind speed, and the availability of high combustible content in the forest floor. Forest fire risk zones are areas where a fire is likely to start and quickly spread to other parts of the forest (Ghobadi et al., 2012).

National Parks are regions of land that are protected by the government for conservation and tourism purposes, usually because of their extreme natural beauty or high biodiversity. Ethiopia is home to several national parks. Simen Mountains National Park is one of the most outstanding natural locations in the world and a prime example of the natural heritage of the world. The SMNP is of international significance, having been designated as a "World Heritage Site" by the UNESCO World Heritage Committee in 1978 due to its vast biodiversity, large number of endemic species, and significant biophysical features. Due to evidence of recent deterioration of the Walia ibex population, agricultural encroachment, loss of biodiversity, and the impacts of road development, the SMNP was inscribed on the list of World Heritage in danger in 1996 (Hassen, 2018).

Currently, forest fires threaten Simen Mountains National Park. A forest fire that broke out in the park in 2019 was difficult to control and devastated a substantial part of the park's grasslands, shrubs and forests. Fire was the type of hazard faced by temperature variation and the surrounding communities. In most fire-prone areas, the occurrence of fire hazards within the

protected area originates from human activity (Chernet & Consult, 2015). The presence of a public road in the core area of the Park, which fragments the park and exposes it to increased human activities and lack of adequate technical skills, also affect proper management of the park and leads to forest fires.

Remote sensing Satellite data is used in different phases of fire management: before the fire, to estimate fire danger conditions; during the fire, to detect active fires and estimate fire behavior, and after the fire, to analyze fire effects and vegetation recovery (Chuvieco et al., 2020). Multi-temporal data acquisition and synoptic viewing capabilities are possible with remote sensing satellites (Alganci et al., 2010). Hence, this study focused on monitoring and mapping forest fire extents by using normalized burn ratio, assessing land use /land cover change dynamics, mapping fire risk models and forecasting the future forest fires of SMNP.

## 1.2. Statement of the Problem

Forest fires have become a major concern for several environmental experts, on a global scale, fire is the most effective means of transforming tropical forests into agricultural areas, and it has severe impacts on the global atmosphere (Yakubu et al., 2015). When forest fire burns in an uncontrolled manner, fire has been a cause of ecosystem disruption. According to Vicente-Serrano et al., (2020) loss of forest, loss of bio-diversity, loss of wildlife habitat, global warming, soil degradation, loss of biophysical wood and fodder, damage to water and other natural resources, and loss of natural regeneration are among the ecological and socio-economic effects of wild land fires. Forest fires are causing significant harm to the environment, human health, properties and putting life at risk. Historically, forest and wild land fires have occurred, affecting the landscape structure, pattern and consequently the ecosystem species composition. The ecological role of fire is to influence several factors, such as plant community development, soil nutrient availability and biological diversity (Roy, 2003).

Wildfires are prevalent almost everywhere in the world these days. If a wildfire occurs, natural resources are burnt away and the wildlife area is destroyed. Accordingly, environmental conditions (i.e., weather, temperature, water quality, etc.) can be changed (Heo et al., 2008).

Though there is no accurate documented data that allows examination of the extent of damage caused by forest fires in Ethiopia, it has resulted in significant economic and biological loss.

SMNP is of global importance for biodiversity conservation as it is home to globally endangered species, including the famous Walia ibex, a rare wild mountain goat, the Gelada baboon and the Ethiopian wolf. Most of the above-described problems are commonly available in SMNP. In this area, the most forest fires have occurred between the months of March and May, when the temperature of the area is at its peak (Chernet & Consult, 2015). In April 2019, there was a forest fire in SMNP and it damaged a large area of the park, but there is no fire statistical data permitting any analysis of the risk and extent of the damage.

Previously, various studies have been conducted related to this research title in other study areas. Among these, Genanaw (2008) and Suryabhagavan et al (2016) used LULC, slope, aspect, elevation, settlement and road proximity to produce a fire risk model and to generate a degradation assessment. Similarly, (Saklani, 2008) and Tafesse (2016) developed and mapped forest fire risk zones using ignition and the biophysical Risk Submodel. Even though the above-mentioned researchers conducted studies related to forest fire risk modeling, in this study, identified and filled gaps are: No related studies have been undertaken in the study area yet and this research used the Difference normalized burn ratio (dNBR) method to determine how much the study area was burned by fire. Moreover, this Difference normalized burn ratio was overlaid with the ignition and biophysical risk models to create the final forest fire risk model. Finally, this research intended to raise awareness for stakeholders and indicate appropriate measures.

## 1.3. Objective of the study

### 1.3.1. General Objective

The main objective of this study is to map forest fire extents and model fire risk Zone of Simen Mountains National Park by using GIS and remote sensing approach.

### 1.3.2. Specific Objective

This research addressed the following specific objectives:

- To monitor and map forest fire loss extents using Difference normalized burn ratio(dNBR)
- To assess land use /land cover change of study area
- To map forest fire risk zone and forecast forest fire risk of the study area

## 1.4. Research questions

- What is the extent of forest fire in SMNP?
- How is the dynamics of land use/land cover in SMNP during different periods?
- How to map fire risk model and forecast future forest fire risk in SMNP?

## 1.5. Significance of the study

SMNP has possessed an area of land with extreme natural beauty or rich biodiversity. However, this national park lost a large area of forests due to forest fires. Hence, assessing forest fire extent and forecasting fire risk is vital owing to the following concerns: It will contribute to understand the application of GIS and remote sensing on forest fire analysis and inform different stakeholders for their decision-making processes regarding fire monitoring. Such maps help forest department officials to prevent or minimize fire risk activities within the forest. Furthermore, the study benefits other researchers who want to study forest fire occurrences through providing insight about the most fire prone areas and factors affecting forest fire in the study area.

## 1.6. Scope of the study

This study was conducted at Simen Mountains National Park and has been carried out to detect and map forest fire extents by using dNBR, preparing land use and land cover maps for the years 2010 (Landsat 7), 2015, and 2019 (Landsat 8). In addition, the study dealt with forest fire risk zone modeling and mapping using biophysical, ignition factors and dNBR by employing GIS and remote sensing approaches.

## 1.7. Organization of the thesis

The present study was organized by including five main chapters: The first chapter of the study is the introduction, which comprises the study's background, statement of the problem, study objective (general and specific objectives), significance, and scope of the study. The literature review was discussed in the second chapter. This chapter introduces several pieces of literature that are relevant to the current study's title and are utilized to provide a brief overview of the theoretical foundations of forest fire mapping, fire risk modeling, GIS, and remote sensing. The third chapter covers a broad overview of the research area, as well as data sources, data

processing, and general methodological flow charts. This chapter provides a detailed description of the study area, including its location, climate, topography, biological diversity and all data, as well as the steps performed to achieve the stated goal. The result and discussion are presented in the fourth chapter. The output of the data analysis technique and thematic data layer maps are presented in this chapter. The fifth chapter discusses the conclusion and recommendations.

# CHAPTER TWO

# 2. Literature Review

In this chapter, there are five sub-sections. These are 1) Basic Concepts and Definitions of Forest Fire, this subsection defines what forest fire is, shows the types and occurrence of forest fire and major causes of forest fire, classified as natural and man-made. 2) The second subsection describes LULC Cover Change Detection, which is used to identify, describe, and quantify differences between images of the same scene at different times or under different conditions. Essentially, it involves the ability to quantify temporal effects using multi-temporal data sets. 3) The third subsection states the contribution of GIS and remote sensing in forest fire monitoring and mapping. This section constitutes different studies conducted using GIS and remote sensing in forest fire monitoring and mapping and displays what the result looks like. 4) Modeling forest fire risk zone: this subsection defines the Biophysical Risk Sub-model, which includes land use/land cover, elevation, slope, and aspect, as well as the Ignition Risk Sub-Model, which includes road and settlement factors that influence the ignition process of fire by providing a conductive environment for fire to ignite. 5) GIS and remote sensing for modeling forest fire; this section shows the involvement of geographic information system, Landsat 8 data and contribution for forest fire monitoring and management.

## 2.1. Basic Concepts and Definitions of Forest fire

Fire is defined as the quick burning of fuel, heat, and oxygen, according to the most popular technical definition. To start a fire, an external source of heat, which is measured in terms of temperature, is required along with oxygen. Fuel can be made from any combustible material, including plants, branches, needles, standing dead trees, leaves, and man-built flammable structures (Saklani, 2008).

### 2.1.1. Forest Fire

The term “forest fire” means fire that is spreading in a forest area, thus burning forest vegetation. Given the national differences in the terms “forest area” and “forest vegetation”, the difference in the meaning of the term “forest fire” is also logical in different countries and regions. Forest fires are described as vegetation fires in specialized literature in the United States, Australia,

Russia, and other countries, as part of the group of so-called "landscape fires," which comprise grasslands, pastures, agricultural areas, and other locations, but not forest areas (Asenova, 2018). Recently, with respect to the analysis of the causes leading to global climate change, so-called natural fires or wildland fire, have also been added as a factor. The so-called "defined fires" also burn plants without stating their type or the practical purpose of the land they cover. Thus, the area covered by the fire includes parks, urban areas, orchards, vineyards, agricultural plantations and other areas covered with vegetation. Using the general terms in forest fire statistics leads to considerable variation in data and incorrectness in comparison and evaluations. According to the European Forest Fire Information System (EFFIS), such data are compiled, i.e., they are specified based on a compilation protocol. For clarity, this work shall use the classic term “forest fire” with the following definition: uncontrolled burning of forest vegetation, which is spread in forest areas and inflicts (causes) direct and/or indirect damage to forests and forestry (Asenova, 2018).

According to Roy (1996), forest fire has intense impacts on the physical environment, including land-use/land-cover, biodiversity, climate change and forest ecosystem. Different researchers have found the part of biomass burning to global budgets of many chemically active gases such as carbon dioxide, carbon monoxide, methane, nitric oxide, methyl chloride and elemental carbon particulate (Genanaw, 2008).

### 2.1.2. Major Causes of Forest fire

A forest fire can be classified based on its origin, into two main categories. These are natural and manmade, in which manmade fires are further classified as intentional and unintentional (Genanaw, 2008; Saklani, 2008). Naturally, forest fire occurs mainly due to lightning or sometimes due to rolling stones and rubbing of dry tress with each other by a strong wind. Lightning is an important source of natural fires, which have influenced savanna-type vegetation in pre-settlement periods. Although some forest fires occur naturally, a combination of human activity, biophysical availability, and climate accounts for the majority of forest fires. Natural forest fire is favored by climate and vegetation cover. Similarly, the high temperatures of tropical and sub-tropical climates combined with a strong wind in the summer season result in natural forest fires (Saklani, 2008). That means the contribution of natural fires is also insignificant in comparison to the number of fires started by humans (Genanaw, 2008).

This problem has mostly affected large forest areas in the USA, Canada, Australia, and European countries (Asenova, 2018).

In addition to natural occurrences, the majority of forest fires occur as the combined effects of human activity, fuel availability, and climatic conditions (Genanaw, 2008). According to FAO (2010) forest fire statistics, humans are the major causes of forest fires at a global level. In this report, it is explained that at least 80 percent of forest fires in the world are caused by people and in some regions, up to 99 percent. Manmade causes are further classified as intentional and unintentional. Mainly, intentional fires occurred in search of better growth of fodder grass (Saklani, 2008), demand for conversion of forest to other land uses (Genanaw, 2008), for timber harvesting, land conversion, slash-and-burn agriculture, and socio-economic conflicts over the question of property and land use rights (FAO, 2010). Unintentionally, a fire occurs in a forest due to the carless throwing of match-sticks and burning ends of cigarettes (Genanaw, 2008). Similarly, the majority of forest fires in Ethiopia are induced by human intentional action to fulfill their temporal needs (MOA, 2000).

## 2.2. Forest Fire Monitoring and management system in Ethiopia

An adequate firefighting organization and management system for fire suppression does not exist. There are no trained and equipped personnel for firefighting and the prevention is mainly through the mobilization of the farming communities. The weak institutional set-up of the sector at all levels to monitor all forested areas and implement preventive measures has limited the prevention mechanisms to be traditional. There are forest protection committees established in each administrative zones but are not functional and effective since there is no budget allocated for fire prevention. The management of forest fires has been poorly organized and uncoordinated. There is no formal unit /institution, which are responsible for forest fire management. It is one of the several responsibilities of the Forestry and Wildlife Technology and Regulatory Team within the ministry of agriculture at the federal level and bureau of agriculture at the regional levels. At the federal level, forest protection, including fire issues falls within the responsibilities of the Forest and Wildlife Conservation and Development Team of the ministry of agriculture. At the regional levels, the regional Bureau of agriculture Development is responsible for forest fire protection. However, there is no special force for fire management. It is only activated when there are emergency fire outbreaks. In such cases, both the urban and rural communities are mobilized.

There are no especially trained personnel, equipment and financial resources. There is no trained crew or organization for firefighting. People are mobilized without training in firefighting and fire fighter safety(Teketay, 2000).

## 2.3. Land-use and land-cover change detection

Land-use and land-cover change is considered as one of the most important environmental issues of global concern. Changes in land use/land cover and the associated habitat loss and fragmentation are major causes of biodiversity loss. Such changes are usually caused by human activities like deforestation, urbanization, farming escalated, overgrazing, and subsequent land degradation (Halmy et al., 2015).

Detection of LULC changes is the process of identifying differences in the state of a pixel or phenomenon by analyzing images acquired on different dates (Viana et al., 2019). Change detection analysis includes a broad range of methods used to identify, describe, and quantify differences between images of the same scene at different times or under different conditions. Essentially, it involves the ability to quantify changes in temporal images using multi-temporal data sets. According to Lillisand and Kiefer (2000), change detection, whether it is a forest or not, involves the use of multi temporal data set to discriminate areas of land cover change between dates. There are various approaches to change detection, which are employed for various applications. These include post classification comparison, classification of multi temporal data sets, principal component analysis, temporal image differencing and temporal image ratio (Lillesand and Kiefer, 2000). Among the various approaches of change detection techniques, post classification comparison change detection is the most commonly used method. It involves the overlay of two or more classified images. Change areas are simply those areas that are not classified the same at different times (Singh, 1989). Detection of changes is used to analyze what land use category is changing to what other type(s) that could be used as baseline information for managerial intervention. Overlay analysis using pixel-to-pixel comparison of the study year images is used to detect dynamics, including the direction of change(s) (Genanaw, 2008).

The application of remotely sensed data has made it possible to study the changes in land cover in less time, at a lower cost, and with better accuracy. it is widely used in updating land use/cover

maps and in land use/cover mapping ("Monitoring Land Use/Cover Change Using Remote Sensing and GIS Techniques," 2015).

## 2.4. Contribution of GIS and RS in Forest Fire monitoring and mapping

Using GIS and remote sensing, several studies are being conducted on forest fire extent mapping, cover change, and modeling of fire risk zones. Some of these investigations are presented in this paper in order to establish a theoretical foundation for the current research.

In the Bale Mountains National Park (BMNP), Oromia, Tafesse (2016) conducted a study on forest fire risk zone modeling and mapping. The study created a forest fire risk model, mapped the BMNP's fire risk susceptibility and attempted to validate the forest fire risk model created in the study area. Using the weighted overlays technique, the study applied the biophysical and ignition sub models. To quantify forest fire risk and identify fire-prone areas, the researchers used remote sensing and a Geographic information system (GIS). In this study, Landsat 8 images were used. In addition to satellite imagery, the research area's Digital Elevation Model (DEM) was created using 30 m resolution SRTM data to determine elevation, slope, and aspect. According to the findings, 94.28 $km^2$ (4.5%), 868.10 $km^2$ (41.55%), 997 $km^2$ (47.73%), and 129.56 $km^2$ (6.2%) of the BMNP are classified as extreme, high, moderate, and low risk, respectively. The current study is intended to include a third factor, Difference Normalized Burn Ratio (dNBR), in addition to the two models.

Genanaw (2008) used GIS and remote sensing to map forest cover change and fire risk susceptibility in the Goba Woreda area. The study produced a map of land use/land cover and forest cover, as well as forecast a forest fire danger zone for the study area. Finally, each factor was multiplied by their respective weights derived from the pairwise comparison and factors, and the final output of forest fire risk susceptibility map was created using the MCE (Multi Criteria Evaluation) approach. According to the result of the study, 18% and 25% of the woreda's total forest are classified as very high and high susceptibility levels, respectively. In the same order, the remaining 35% and 21% are classed as moderate and low levels. The new study addressed a gap similar to the previous study reported in Tafesse (2016), which used additional criteria by producing a previous fire risk map.

Using GIS and remote sensing tools, Adab et al. (2013) investigate forest fire risk in northeast Iran. The inputs used include vegetation moisture, height, slope, aspect, distance from settlement and roads to calculate forest fire risk. The model performed properly, but more research should be done by including new variables such as previous fire spot areas and land use land cover to make more accurate model.

Sunar & Özkan (2001) studied forest fires with remote sensing data. GIS was established to monitor and predict the extent of the damage, and to enhance fire management efficiency. The database was designed for use in a GIS environment. A database was implemented in GIS to analyze forest first risk. Digital image processing methods, such as spectral profile analysis, vegetation indices and multispectral classification were applied to the satellite sensor images acquired before and after the forest fire. The crucial factors of ignition and biophysical risk model, however, were not used to estimate the future fire extent. Filippidis & Mitsopoulos (2004) investigated the use of historical fire data to map forest fire risk zones. The study used risk analysis elements such as vegetation types, height, slope, and aspect that affect fire behavior characteristics. Following the statistical analysis, five classifications of forest fire risk zones were automatically generated, ranging from very high to very low. The study found that the influence of fire behaviors was insufficient to establish forest fire risk zones and that the closeness of roads and settlements, as well as the prior fire risk region, were not taken into account and did not show the model map clearly.

## 2.5. Normalized Burn Ratio (NBR)

The Normalized Burn Ratio (NBR) was formulated as an index to detect burned areas. In recent years, NBR has frequently been used to identify burn areas and burn severity (Chen et al., 2011). It is presented as a reliable means to map fire severity, computed as the difference between near infrared (NIR) and short wave infrared (SWIR) reflectance divided by their sum. These bands are used because they present the best contrast between photosynthetic healthy vegetation and burned vegetation. Besides that, there is an increase in MIR band reflectance due to decreased water absorption by the canopy, followed by a decrease in NIR reflectance that can be seen in burned areas (Vedovato et al., 2015). The normalized burn ratio (NBR) has become accepted as the standard spectral index to estimate fire/burn severity (Veraverbeke et al., 2010). Initially designed for burned area extraction, NBR is the most popular spectral index used for burn severity

assessments with different sensors in several ecosystems around the world (Fornacca et al., 2018). According to Polychronaki & Gitas (2012), the NBR is defined as follows:

$$NBR=\frac{NIR-SWIR}{NIR+SWIR} \quad (1)$$

NBR can theoretically range from +1.0 to −1.0 and negative values are assumed to represent burned pixels, with fire severity increasing as NBR values become more negative.

In the United States, normalized burn ratio (NBR) and Difference normalized burn ratio (dNBR) are commonly used to assess landscape-scale post-fire effects (Lentile* et al., 2006). By using the following equation, dNBR is often used as a basis to evaluate the potential of remote sensing indices for assessing burn severity (Fang & Yang, 2014).

$$dNBR = NBRpre - NBRpost \quad (2)$$

Where, dNBR is Difference Normalized Burn Ration, NBRpre is Pre Fire Normalized Burn Ratio, NBRpost is Post Fire Normalized Burn Ratio.

## 2.6. Modeling of Forest Fire Risk Zone

### 2.6.1. Biophysical Risk

Land use land cover, elevation, slope, and aspect are all included in the Biophysical Risk Sub-model. The most critical factors that will determine the location where a fire is likely to start are topographical and land use characteristics (Tafesse, 2016).

#### 2.6.1.1. Elevation

Because elevation affects precipitation and temperature, it is considered an influencing element in forest fire. Rainfall tends to increase as the elevation rises. As a result, higher elevations have a lower risk of fire. In terms of temperature, higher elevation leads to a lower temperature, which means there is a decreased chance of fire in higher elevation places (Yakubu et al., 2015). Elevation above sea level has an impact on the general climate and, as a result, on biophysical availability. Because of differences in precipitation, snowmelt dates, and green-up and curing dates, the length of the fire season and the amount of biophysical available varies with elevation (Yakubu et al., 2015). Elevation is an important physiographic characteristic that is linked to temperature, humidity, and wind. As a result, it plays a crucial role in the spread of fire (Adab et al., 2013).

#### 2.6.1.2. Aspect

The aspect of a slope is the direction in which it is facing. Aspect influences fire behavior by varying the amount of solar energy and wind received by different aspects (Adab et al., 2013; Yakubu et al., 2015; Adab et al., 2013; Yakubu et al., 2015). When the slope is perpendicular to the sun's angle, the solar radiation intensity is highest. Fuels on slopes with an easterly face will dry out early in the day in the northern hemisphere, but not as quickly as fuels on slopes with a westerly aspect. It can be deduced that the slope, which faces the wind direction, is easier to cause a raging fire. A north-facing slope also receives less sunlight than a south-facing slope. As a result, southern faces receive more direct sunlight, which dries the soil and vegetation (Yakubu et al., 2015).

#### 2.6.1.3. Slope

Among the topographic elements, slope is particularly essential. Slope has a significant impact on the speed with which a fire spreads. Fire always spreads faster uphill than it does downhill. The intensity of radiation and the moisture content of the fuels are also affected by the slope steepness. The slopes where the fuel is the driest vary with time of year, time of day, and latitude. Because of the differences caused by the varying amounts and intensities of solar radiation received, the behavior of a fire as it spreads across the landscape can be predicted to be influenced by the time of day and topographic factors. The slope has a big impact on the forward rate of spread of surface fires because it changes the degree of preheating of the unburned fuel in front of the flames. This is accomplished in a head fire by altering the flames to a highly acute angle and with slopes surpassing 15-20°C; the flame propagation process entails practically constant flame contact, just as it is with the wind. Conversely, a downslope decreases the rate of spread of surface head fires. Steep slopes increase the speed of fire a lot because convective preheating and ignition rates are more effective. In other words, a larger slope of the terrain will lead to a larger probability of causing a fire (Yakubu et al., 2015).

#### 2.6.1.4. Vegetation and Fuel

Vegetation type has a strong relationship to forest fire risk. Different types of vegetation have different kinds of combustibility (Syphard et al., 2007). Because coniferous trees contain less,

water and are oilier than deciduous trees, coniferous forests have a higher risk of fire than deciduous forests. Fuel is an important component of both the fire fundamental and fire environment triangles: Fuel, oxygen, and heat in the fire fundamental triangle, and fuel, terrain, and weather in the fire environment triangle. Fuel does not start a fire, but it does modify the way it burns, affecting the ease with which it starts, as well as the size and intensity of the fire. Fuel can be described in terms of both fuel state and fuel type. The moisture content of the fuel whether it is alive or dead are referred to as a fuel state. Fuel type is a description of the fuel itself. The description of fuel the type includes the physical properties of the fuel, fuel components and fuel complexes (Yakubu et al., 2015). Fuel properties that affect the way the material burns include quantity, size, compactness, and arrangement. Fuel components, which are related to the way vegetation grows, may be specified as ground, surface and crown biophysical components as well as grass, litter, brush, or over the story. Biophysical complexes, which are associations of components, include grass and timber, along with grass and litter understory. Moisture content, expressed as a fraction, is the mass of water held by the unit mass of oven dry biophysical and is determined primarily by biophysical type and weather. It may also be expressed as a percentage of the fuel oven dry weight. Fuel moisture is normally expressed on a dry matter basis and is a critical factor in determining the intensity of a fire because it affects the ease of ignition, the quantity of biophysical consumed and the combustion rate of the different types of biophysical. The most important influence of biophysical moisture on fire behavior is the smothering effect of the water vapor released from the burning biophysical. It reduces the amount of oxygen in the immediate proximity of the burning plant material, thus decreasing the rate of combustion. Fuel load is regarded as one of the most important factors influencing fire behavior because the total amount of heat energy available for release during a fire is related to the quantity of fuel. Assuming a constant heat yield, the intensity of a fire is directly proportional to the amount of fuel available for combustion at any given rate of spread of the fire front (Yakubu et al., 2015).

### 2.6.2. Ignition Risk

The Ignition sub-model includes road and settlement factors. These factors influence the ignition process of fire as it provides a conductive environment for fire to be ignited. Different studies related to human factors affecting fire occurrence found that distance from the road and distance from settlements are significant (Tafesse, 2016). The ignition model is related to human

activities like careless use/disposal of cigarettes, fireworks, and campfires. Human settlement areas and agricultural areas where slash and burn farming practices occur were identified as the firebrand. The closer the biophysical is to the firebrand, the higher the ignition risk (Suryabhagavan et al., 2016).

## 2.7. GIS and Remote Sensing for Modeling Forest fire

### 2.7.1. Geographic Information Systems (GIS)

There are many different definitions for GIS, but the basic concept common to all definitions is that GIS is a set of programs that store, manage, manipulate and represent data with some kind of spatial components. A Simple definition of GIS is that it is an organized collection of computer equipment, programs, and geographic information outlined to proficiently capture, upgrade, control, analyze, and show al1the shapes of topographically referenced data (Dangermond, 1992). Moreover, procedures are designed to support capture, manage, manipulation, analysis, modeling and display of spatially referenced data to solve complex planning and management problems (Shiferaw & Suryabhagavan, 2019).

GIS was established to monitor and predict the extent of the damage, and to enhance fire management efficiency. In recent years, GIS has been used as a powerful tool in combination with multi temporal remote sensing data for studying and monitoring the impact of many environmental factors. Many government agencies now use a wide range of computer-based information systems to handle geographic aspects of their business, particularly mapping, by integrating spatial data collected from different sources, and in different formats, into GISs (Sunar & Özkan, 2001).

## 2.8. Landsat 8 Data and Contribution for Fire Monitoring

The National Aeronautics and Space Administration (NASA) launched Landsat 8 in 2013. The Operational Land Imager (OLI) and Thermal Infrared Sensor (TIRS) are on board Landsat 8. The OLI collects data in the visible, panchromatic band, and short-wave infrared spectral bands, while the TIRS collects images in the thermal range. Landsat 8 data is open to the public and has been widely used by researchers for several applications. Agriculture, forestry, and range resources, as well as land use and mapping, geology, hydrology, coastal resources, and environmental monitoring, all used Landsat (Schroeder et al., 2016). A multi-spectral satellite sensor measures

emitted or reflected electromagnetic radiation, or spectral properties, from a target object in remote sensing (Shiferaw & Suryabhagavan, 2019). With the ability to detect and monitor vegetation biomass in greater detail than estimated ground estimates, remote sensing enables more objective, definite, and unbiased judgments to be made from a synoptic viewpoint (Asenova, 2018).

For risk estimation, identification, and assessment, remote sensing technology was used in various stages of fire control. For post-fire damage analysis, remotely sensed data provides fast, accurate, and reliable information. Remote sensing satellites are capable of multi-temporal data collection and synoptic viewing (Alganci et al., 2010).

In addition to agriculture and forestry, Landsat 8 data has been used to monitor changes in land cover and land use, as well as for mapping. Landsat_8 can collect data in a variety of spectrums, including visible (VIS), near infrared (NIR), short wave infrared (SWIR), and a panchromatic band with a wavelength range of 0.4-2.5 m. On the other hand, TIRS collects images in the thermal region at 10–12.5 μm spectrums (Ridwan et al., 2018). The characteristics of OLI/TIRS are shown in the (Table 1).

Table 1. OLI/TIRS bands and their characteristics

| Sensor | Band Number | Band | Wave length | Resolution (m) |
|---|---|---|---|---|
| OLI | 1 | Coastal/aerosol | 0.435-0.451 | 30 |
| | 2 | Blue | 0.452-0.512 | 30 |
| | 3 | Green | 0.533-0.590 | 30 |
| | 4 | Red | 0.636-0.673 | 30 |
| | 5 | Near infrared | 0.851-0.879 | 30 |

| | | | | |
|---|---|---|---|---|
| | 6 | SWIR1 | 1.566-1.651 | 30 |
| | 7 | SWIR2 | 2.107-2.294 | 30 |
| | 8 | Panchromatic | 0.503-0.676 | 15 |
| | 9 | Cirrus | 1.363-1.384 | 30 |
| | 10 | TIRS1 | 10.6-11.19 | 100 |
| TIRS | 11 | TIRS2 | 11.50-12.51 | 100 |

Source: (Ridwan et al., 2018).

# CHAPTER THREE

# 3. MATERIALS AND METHODS

## 3.1. Description of the study area

SMNP is located in the North Gondar Administrative Zone, Amhara National, Regional State, in the northwest of Ethiopia. Geographical location of this area extends from 13º06'44.09" N to 13º23'07.85" N latitude and 37º51'26.36"E to 38º 29'27.59"E longitude (Fig. 1). It covers an area of 412 $km^2$ and is bordered by five districts of the Zone (Debark, Janamora, Adiarikay, Beyeda, and Telemit). It is located 120 km northeast of Gondar town and 860 km faraway from Addis Ababa. (Masresha, 2019)

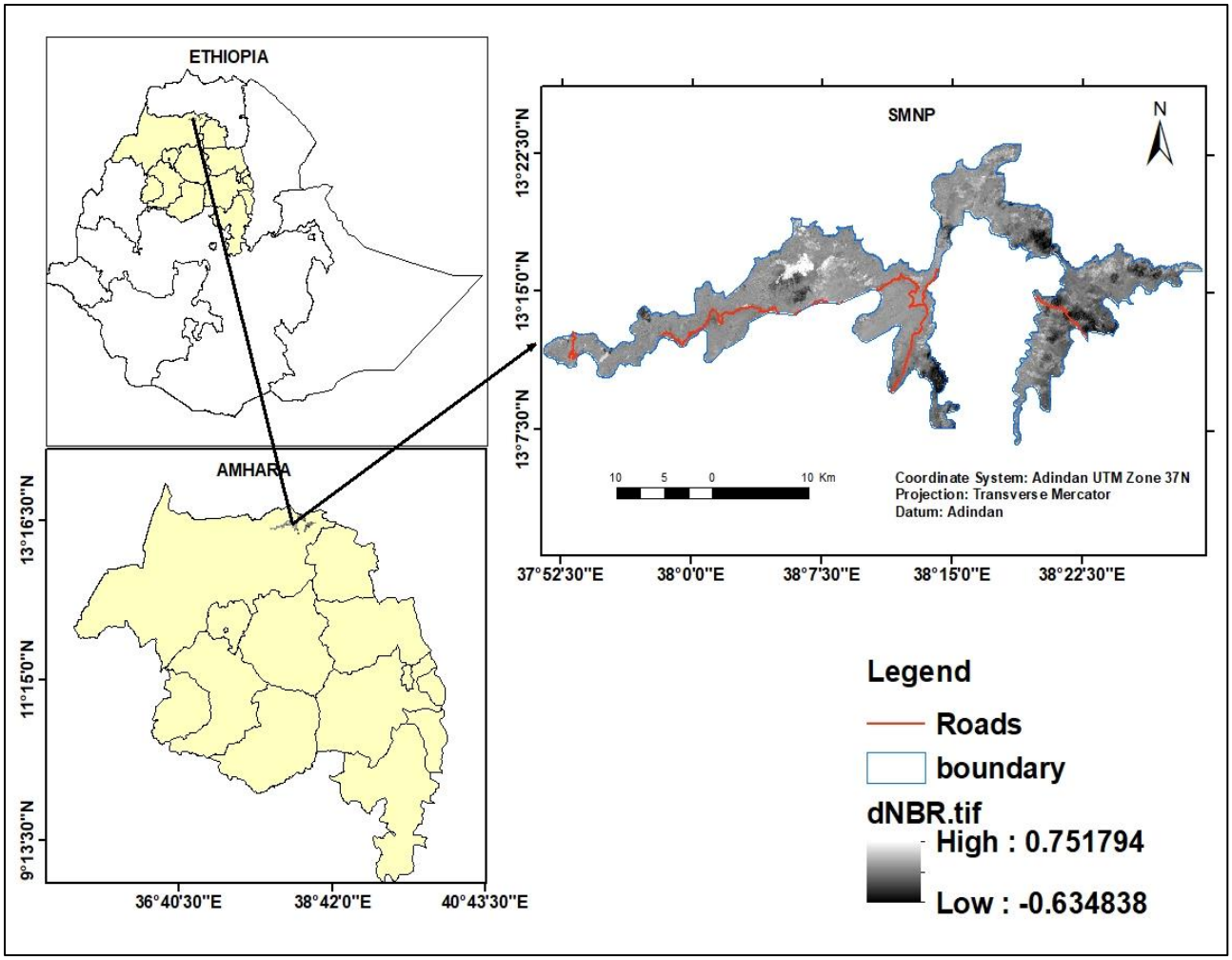


**Fig. 1.** Location map of the study area

### 3.1.1 Climate

The Simien Mountains have a wet and dry season, and obtains nearly 75 percent of the yearly precipitation between June and September. The annual rainfall amount of SMNP is between 1350-1600 mm, with an annual average of rainfall of around 1,500 mm at 3,600 m a.s.l (Hassen, 2018). The temperatures of the area are relatively constant throughout the year; however, there is huge variation starting from a minimum of -2°C to -4 °C in the nighttime to a maximum of 11°C to 18°C during the day. The Simien Mountains' climate is divided into four altitude-based climatic zones: alpine climate (Wurch zone) is above 3,700 masl, chilly climate (High Dega zone) from 3,400 to 3,700 masl, temperate temperature( Dega zone) is from 2,400 to 3,400 masl and tropical climate( Woina Dega zone ) from 1,500 to 2,400 masl) (Hassen, 2018).

### 3.1.2 Topography

The Simien Mountains scene is comprised of the Simien Mountain massif, adjacent forest areas and the surrounding community lands in northern Ethiopia. Characteristics of the area are its topographical roughness with steep escarpments, rolling hills in the highlands and flat terraces dissected by rivers in the lowlands. The massif was formed some 25 million years ago and the igneous basalts have since been eroded to form precipitous cliffs and deep gorges. A few cliffs reach 1,500 m in height and extend for long distances. SMNP is one of the major highlands of Africa. The Simien Mountains are the most elevated parts of the Ethiopian Plateau (more than 2,000 meters; 6,560 feet). They rise to the highest point in Ethiopia at Ras Dejen (4,543 m a.s.l), the fourth highest peak in Africa ( https://whc.unesco.org/en/news/1482/).

### 3.1.3 Biological Diversity

In 1978, SMNP was designated as a World Heritage Site due to its huge quantity of endemic species, distinctive biophysical features, and international significance. (Yihune et al., 2009). The Park is known for endemic wildlife species, such as the Walya Ibex and the Simien fox (Ethiopian wolf). The natural vegetation belts are typical of Ethiopia where most extended vegetation sequences are seen in their altitudinal range. Due to the decline of the Walia Ibex population, agricultural encroachment from surrounding weredas, and the effects of road building, the park was listed on the list of World Heritage in Danger in 1996. According to Ethiopian Wildlife Conservation Authority (EWCA), 2014 report, the park is gifted with floristically rich vegetation growing in four belts related to altitude: Afromontane forest, Hypercom woodland, Afromontane grassland and Afro-alpine moorland. These include species in the latter two biomes showing adaptations to extreme high-altitude conditions, and much speciation. However, the heavy overgrazing has eroded and degraded the grassland. Now SMNP is a mountainous area endowed with unique botanical and zoological combinations that have been able to resist human interference because of the extreme topography and altitudinal range of the landscape (Hassen, 2018).

## 3.2. Data Source and Methods of Data Collection

### 3.2.1. Data Source and Description

For this study, data was collected from different sources. The satellite imageries and other data used in this study are summarized in the following Tables 2 and 3.

**Table 2.** Data type and sources used in the study

| No | **Data** | **Purpose and description** | **Source** |
|---|---|---|---|
| 1 | SRTM DEM | For mapping the elevation, aspect and slope of the area | https://earthexplorer.usgs.gov/ |
| 2 | Landsat 8 OLI and Landsat 7 ETM+ | For LULC, identify and monitor burnt area (Using NBR and dNBR) | https://earthexplorer.usgs.gov/ |
| 3 | Point data (x,y) | For model validation and accuracy assessment | From google earth pro |
| 4 | Shape files ( Boundary, Settlements and roads | To identify the boundary and ignition risk model | Ethiopian geospatial agency |
| 5 | Previous studies, journals, published books | To execute the objectives and for literature review | Secondary sources, internet, library... |

**Table 3.** Input satellite images

| Image | Sensor | Path/row | Pixel size(resolution) | Date of acquisition |
|---|---|---|---|---|
| Land sat 7 | ETM+ | 169/051 | 30 ×30 | 27/03/2010 |
| Land sat 8 | OLI | 169/051 | 30×30(for band1-7 and 9) | 18/04/2015 |
| | | 169/051 | 30×30(for band1-7 and 9) | 13/04/2019(post fire)<br>24/02/2019(pre fire)<br>for NBR and dNBR |

**Source:** Metadata of downloaded Landsat images

### 3.2.2. Software and Tools Used

The following soft wares are used for data analysis that are very vital for the achieving the objectives of the research efficiently and effectively (table 4).

**Table 4.** Software & tools

| No | Software & tools | Purpose and description |
|---|---|---|
| 1 | Arc GIS | For fire risk map preparation and to produce factor maps of forest fire-risk were reclassified and standardized<br>For calculation of NBR and dNBR using raster calculator |
| 2 | ERDAS imagine 2015 | To process satellite image enhancement, pre-processing, image classification to produce LULC map and accuracy assessment |
| 3 | IDRISI SELVA 17.0 | For pairwise comparison/ weight decision analysis |
| 4 | Google earth | To interpret images which is not clear on Landsat 7&8 image and to generate x y coordinates for accuracy assessment. The date of google earth and temporal Landsat images were similar.<br>To collect validation (x, y) points of burned area in a similar time of Landsat images |
| 5 | MS Excel , word and Power point | To create word Document and presentation, data calculation, graph and point coordinates data preparation. |

## 3.3. Methods of data analysis

### 3.3.1. Forest fire loss extent of SMNP

The Normalized Burn Ratio (NBR) and the difference in the Normalized Burn Ratio between pre- and post-fire images (dNBR) are widely used to infer fire severity from remotely sensed data (Lentile et al., 2006). In this study, the recent forest fire losses in SMNP was evaluated and quantified using the difference of pre and post fire normalized burn ratio. The Normalized Burn Ratio (NBR) is a burn detection index. It's described as a reliable way to map fire severity, and it's calculated by dividing the difference between Near Infrared (NIR) and Short-wave Infrared (SWIR) reflectance by their sum.(Vedovato et al., 2015). In the current study ArcGIS 10.4, raster calculator used to calculate the normalized burn ratio (NBR) and difference normalize burn ratio

(dNBR). Landsat 8 satellite image of band 5 and 7 was used to generate the normalized burn ratio (NBR) by using the following equation (Rodriguez, 2021) and (Tran et al., 2018):

NBR = (NIR- SWIR2)/ (NIR+SWIR2) (3)

where NIR (Near Infrared) as a band 5 and SWIR2 (Short Wave Infrared 2) as a band 7. NBR values can potentially range from +1.0 to -1.0, with negative values indicating burned pixels and increasing fire severity, as NBR values get more negative (Fig.2 and 3).

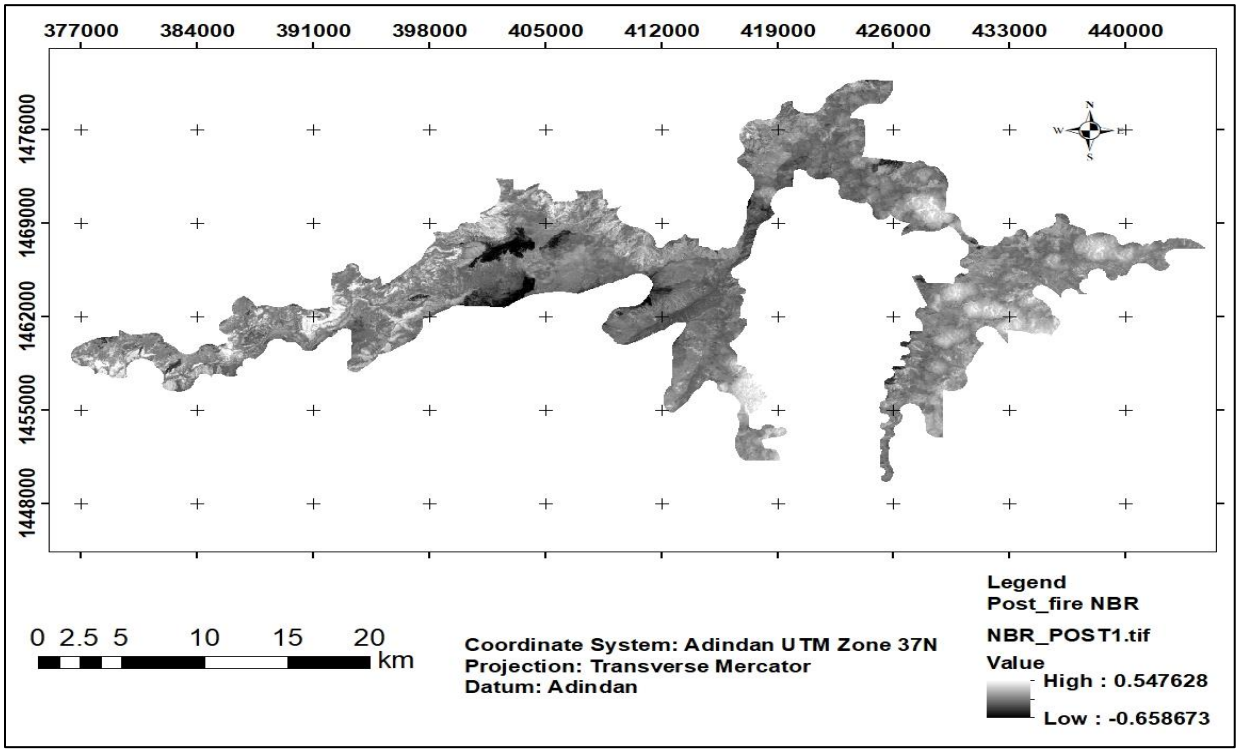


**Fig. 2.** Post fire normalized burn ratio (NBR) index map

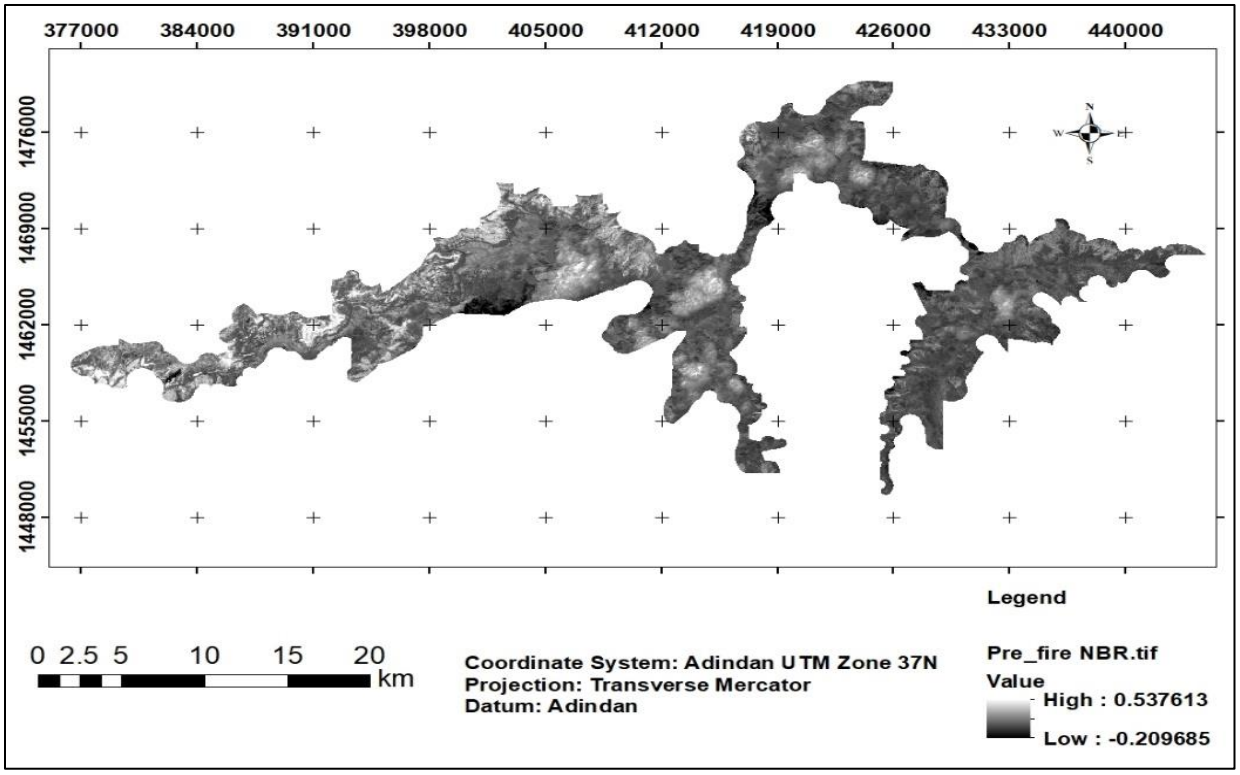


**Fig. 3.** Pre fire normalized burn ratio (NBR) index map

The Difference Normalized Burn Ratio (dNBR) derived from Landsat is one of the more commonly accepted methodologies for assessing burn severity in diverse forest ecosystems (Fang & Yang, 2014). The difference between pre-fire and post-fire NBR (dNBR) is an indication of the spectral changes due to fire. The values of dNBR ranges from -2 to and 2, with positive values indicating burnt pixels and increasing fire severity, as dNBR values get more positive (Melchiorre & Boschetti, 2018). Difference normalized burn ratio (dNBR) formula was calculated using the following equation (Roy et al., 2006).

$$dNBR = NBR_{Prefire} - NBR_{Postfire} \quad (4)$$

According to Rodriguez (2021), the current study was conducted by classifying burn severity levels of dNBR in to four; high, moderate, low and unburnt. The dNBR burn map shows the areas characterized by control point values, which recorded the highest levels of burn severity (Table 5).

**Table 5.** Difference normalized burn ratio (dNBR) burn severity levels and ranges

| dNBR Value ranges | Burn severity levels |
|---|---|
| 0.44 - 0.79 | High severity |
| 0.27- 0.44 | Moderate severity |
| 0.10 - 0.27 | Low severity |
| -0.10 – 0.10 | Unburned |

Source: (Rodriguez, 2021)

### 3.3.2. Analysis of land-use and land-cover change dynamics

#### 3.3.2.1. Image Preprocessing

Image preprocessing is required before using the raw digital satellite image for the desired purpose. It involves procedures that are usually completed before the main data analysis and information extraction. These include atmospheric correction, image rectification and restoration, image enhancement, data merging, GIS integration, and image classification (Genanaw, 2008). The first step in any image processing is to find adequate satellite imagery. Landsat7 images from 2010 (ETM+) and Landsat_8 images from 2015 (OLI) and 2019 (OLI) were used in this study.

#### 3.3.2.2. Atmospheric Correction

Unfortunately, aerosols, clouds, and cloud shadows severely pollute a large amount of imagery (De Keukelaere et al., 2018). Atmospheric correction is critical in overcoming such issues. In order to get land surface attributes from satellite data, atmospheric correction (AC) is required. The effect of the atmosphere contaminates a surface reflectance signal collected by passive satellite instrument. Rayleigh and Mie scattering, the creation of thin cirrus clouds, and gas absorption are some of the mechanisms that prevent one from seeing the surface behind a hazy image of reflected radiation. Atmospheric correction is a method for removing the impact of these processes on a signal that has been measured (Vermote & Kotchenova, 2008). ERDAS IMAGINE image-processing software has an add-on module for atmospheric correction called ATCOR. The outcomes of the haze removal and atmospheric correction utilizing ATCOR yielded good visual result (Neubert & Meinel, 2005). In the current study ATCOR model was used to clear up the blurred images.

### 3.3.2.3. Correction of Scan Line Error

On May 31, 2003, the scan line corrector (SLC) on the Landsat 7 Enhanced Thematic Mapper Plus (ETM+) failed, resulting in wedge-shaped scan-to-scan gaps in the scanning pattern(Storey et al., 2005). With the SLC turned off, the ETM+ continues to collect data, resulting in images that are missing around 22% of the regular scene area (Storey et al., 2005) . To improve the utility, the current study fix scan line error by downloading and adding Landsat toolbox extension into GIS ArcMap10.4. The Landsat toolbox used to eliminate the scan gaps present in a single SLC-off scene and develop scan gap-free imagery. The final processing result looks like the following (Fig. 4).

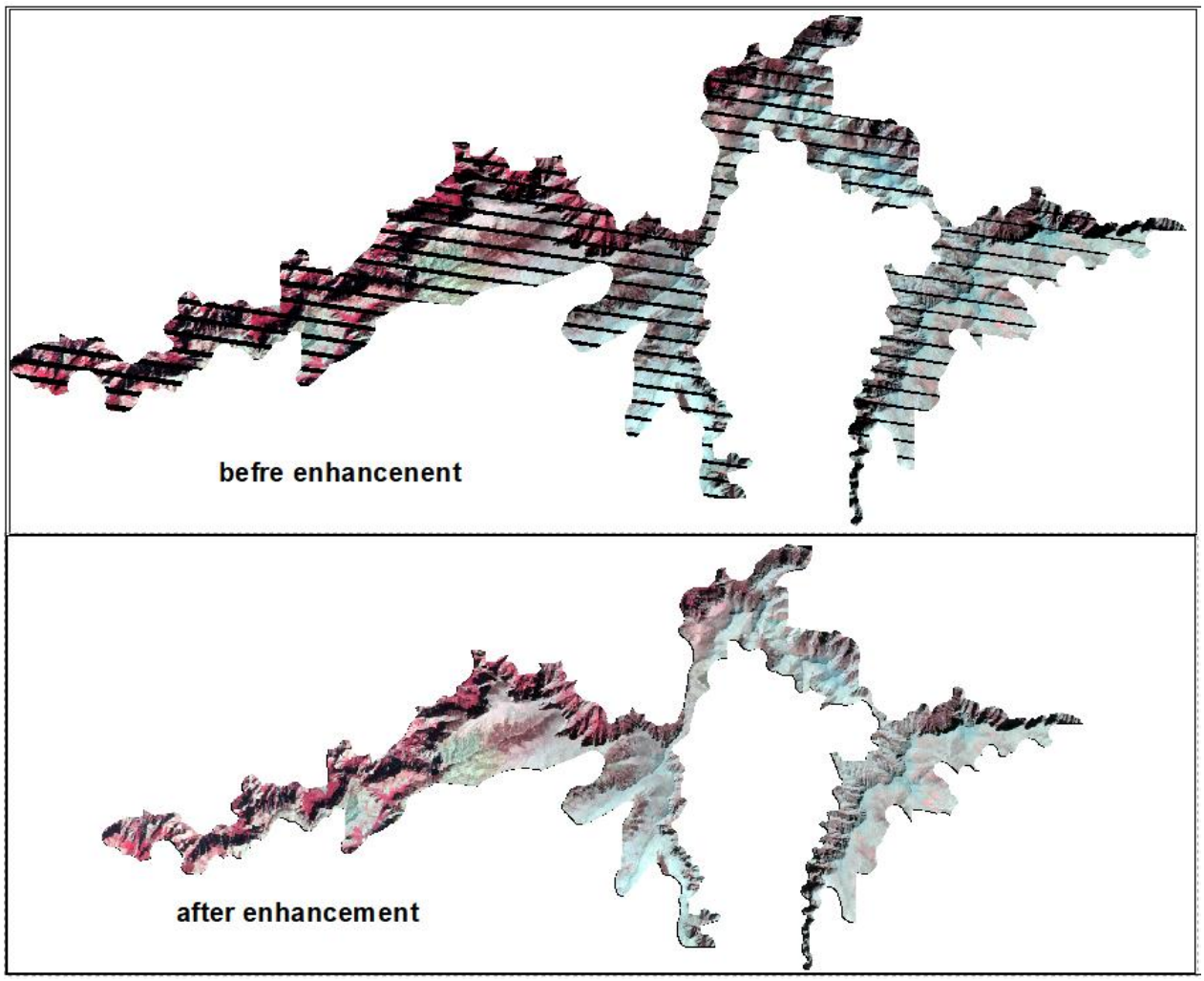


**Fig. 4.** Before and after enhancement of Landsat 7 image

#### 3.3.2.4. Image Classification

In this study area, the following land use land cover classes were identified: shrubs, forest, grassland, farmland, settlements, bare land, rocks, and their description presented in the following way (Table 6).

**Table 6**. Land cover classes of the study area

| LULC class | Description |
|---|---|
| Shrubs | These include shrubs, bushes and young tree species. |
| Forest | These are Afromontane forests comprising natural forests and woodlands with a composition of different tree species and one dominating species (Ericaceous species, of the mix). |
| Grassland | In SMNP, it is also called "Guassa" covered with grassland mixed with Lobelia species used for wildlife grazing and habitat. |
| Farmland and settlements | Areas used for crop cultivation and the scattered rural settlements that are closely associated with the cultivated fields. These were combined into one category, as it was difficult to identify the dispersed rural settlements and a small town as a separated LULC type where fragmented cultivated land exists around homesteads. |
| Bare land | This includes areas covered by soil, sand and rocks. |

Extracting information classes from a multiband raster image is referred to as image classification. Thematic maps can be created using the raster that results from image classification. Depending on the interaction between the analyst and the computer during classification, there are two types of classification: supervised and unsupervised image classification. In the current study, maximum likelihood supervised image classification is preferred to extract and represent training samples. The maximum likelihood classifier dramatically reduces processing times for large scenes. Maximum likelihood classification is a robust technique and there is very little chance of misclassification (Sisodia et al., 2014). Supervised classification is the essential tool used for extracting quantitative information from remotely sensed image data. Image classification has been done using ERDAS 2015 image processing software. By opening the Google earth application, simultaneously with ERDAS image 2015, obtaining more clear information about the

ground truth image for each respective land cover and land use type. For each LULC type over the three years, the number of selected training samples for the study areas was presented in the following (Table 7).

**Table 7**. Signature training samples

| LULC types | Signature Editor training sample value | | |
|---|---|---|---|
| | LULC 2010 | LULC 2015 | LULC 2019 |
| Forest | 57 | 56 | 58 |
| Shrubs | 52 | 51 | 52 |
| Grassland | 55 | 52 | 95 |
| Farmland and settlement | 53 | 55 | 88 |
| Bare land and rocks | 54 | 53 | 55 |
| Total | 271 | 267 | 348 |

Finally, the rate of land use and land cover change dynamics are calculated by using the following formula:

$$r = \frac{Y2-Y1}{T} \quad (5)$$

where, r is Rate of Change, Y2 is Recent year forest cover in ha, Y1 is Initial Year forest cover in ha and T is Interval year between Initial year and Recent year (Berhan, 2007).

#### 3.3.2.5. Accuracy Assessment of LULC Classification

Accuracy assessment is essential for each classification if the classification data is to be useful in change detection. For the accuracy assessment of land cover, maps were extracted from Landsat images. For the three years, 251, 254 and 257 coordinate points were collected at random from images of 2010, 2015, and 2019 on Google Earth respectively to assess accuracy. Then the kml file which was produced from Google earth was converted to a layer file and a point shape file was created to generate x and y coordinates by using ArcGIS 10.4. The imagery on Google Earth and Landsat acquisition dates are similar with identified land use in different periods. Finally, utilizing these processed points, ERDAS IMAGINE 2015 was used to test the accuracy.

### 3.3.3. Modeling Fire Risk Zone Using Weighted Overlay Multi Criteria Analysis

Each data set was categorized into a common scale before using MCE to determine forest fire risk vulnerability. According to Tafesse (2016), the study used ArcGIS spatial analyst tools to assign a discrete, integer value of 1 to 4 to each range. The two models, biophysical risk and ignition risk sub models were produced using the weighted overlay analysis method. A pairwise comparison matrix was computed by IDRISI SELVA 17.0 to resolve personal bias in weight decisions for each dataset. Finally, each factor was multiplied by their respective weights obtained from the paired-wise comparison of the factors and the final output of the forest fire risk vulnerability map was prepared.

#### 3.3.3.1. Producing Biophysical Risk Sub Model

One of the most essential models is the biophysical risk sub model, which contains LULC, slope, aspect, and elevation (Ashiagbor & Laari, 2013). Using the Spatial Analyst tool in ArcGIS10.4, standard topographic maps at a scale of 1:243000 were digitized and the DEM, slope, and aspect parameters for the research area were extracted. The spatial analyst tools in Arcmap10.4.1 were used to calculate elevation, aspect, and slope from SRTM 30m resolution DEM data. The output projection coordinate system was Adindan UTM Zone 37. Then the factor maps are re-classified for assigning weights. Weights have been given to each factor (LULC, elevation, slope and aspect) according to their influence on fire behavior.

Elevation is considered as an influencing factor of forest fire, because elevation relates to precipitation and temperature. In general assumption, with the increase in elevation, rainfall usually increases. According to Teketay (2000) fire behavior in different ecological zones of Ethiopia, in the coldest highlands ("wurch" or "kur") the risk of fire hazard is very low or completely absent. In the cool highlands ("Dega") more or less even distribution of rainfall, which reduces the risk of fire hazard in this zone. Because of sufficient fuel accumulation and strong winds, the distribution of fire becomes so rapid in the event of its outbreak. In the warm highlands ("Woina Dega"), fire hazard may be high owing to dryness of the area, assisted by a wind that also dries the fuel and spreads fire, the grass and other biomass burns faster. In hot ("Kolla"), the spread of fire could be very rapid, and at times difficult to control.

The study area includes zones coldest highlands (Wurch), cool highlands (high Dega), Dega and warm highlands (Woina Dega) (Hassen, 2018).

The elevation of the study area extends from the lowest point at 1752 to 4529 m a.s.l. Therefore, the study has been conducted according to fire susceptibility behavior mentioned above.

Slope is an extremely significant factor among topographic factors. Slope has large effect on the speed of fireside when it is spreading. Fire always spreads faster up-slope than down-slope. Steepness of the slope also influences the strength of the radiation and the fuel moisture. The slopes where the fuel gets the driest vary with year length, day length, and latitude. Thus, as a fire moves over the landscape its behavior can be expected to change with time of day and topographic characteristics because of the variations brought about by the different amounts and intensity of the solar radiation received. Larger terrain slope can give rise to a greater likelihood of causing fire.

Aspect affects fire behavior through variations in the amount of solar radiation and wind that different aspects receive. These aspects receive more sunlight, thus have lower humidity, and higher biophysical temperatures. When the slope is perpendicular to the sun's angle, the solar radiation intensity is highest. Sloped fuels with an eastern aspect can dry out earlier in the day in the northern hemisphere, but not as quickly as those with a western aspect. A slope facing north always receives less sunlight than a slope facing south. Thus, Southern aspects receive more direct heat from the sun, drying both the soil and the vegetation (Yakubu et al., 2015). The current study have been undertaken accordingly.

In this study land use and land-cover was also used as a parameter to form Biophysical Risk Sub Model. Vegetation feature has a strong relationship with the forest fire risk. Different types of vegetation have different kinds of combustibility. Coniferous forest typically has a higher fire risk possibility than deciduous forest, because coniferous trees contain less water and higher oiliness. Fuel components, which are related to the way vegetation grows, may be specified as ground, surface and crown fuel as well as grass, litter, brush, or over story. Grass and timber with grass and trash understory are examples of fuel complexes, which are associations of components (Yakubu et al., 2015). Annual crops, evergreen oak woodlands, eucalypt plantations, pine stands, shrub areas, and grassland are the land cover categories that are ranked according to their fire proneness, from least to most fire prone (Barros & Pereira, 2014).

Annual and perennial crops were the least prone to fire. For the remaining land covers, there seemed to be a gradient of increasing susceptibility to fire from agro-forestry systems (less susceptible) to mixed forests of conifers (or eucalyptus) and broadleaves. Using the most recent (2019 land use/land cover) data, the current study attempted to determine the study area's fire proneness. To produce the biophysical risk sub model the four factors; LULC, elevation, slope and aspect are re-classed in to four fire sensitivity classes (Table 8 and Fig. 5).

**Table 8.** Factors of Biophysical risk sub model

| No | Factors | Classes | Rank | Fire sensitivity |
|---|---|---|---|---|
| 1 | LULC (2019) | Grassland | 1 | Very high risk |
| | | Shrubs | 2 | High risk |
| | | Forests | 3 | Moderate risk |
| | | Farmland & settlement | 4 | Low risk |
| | | Bare land and rocks | 4 | Low risk |
| 2 | Elevation(m) | 1752-2400 | 1 | Very high |
| | | 2400 -3400 | 2 | High risk |
| | | 3400 – 3700 | 3 | Moderate risk |
| | | >3700m | 4 | Low risk |
| 3 | Slope(degree) | >45 | 1 | Very high risk |
| | | 30-45 | 2 | High risk |
| | | 15-30 | 3 | Moderate risk |
| | | 0 -15 | 4 | Low risk |
| 4 | Aspect | West | 1 | Very high risk |
| | | East | 2 | High risk |
| | | South | 3 | Moderate |
| | | North | 4 | Low risk |

Source: (Barros & Pereira, 2014), (Hassen, 2018), (Teketay, 2000), (Tafesse, 2016) and (Yakubu et al., 2015)

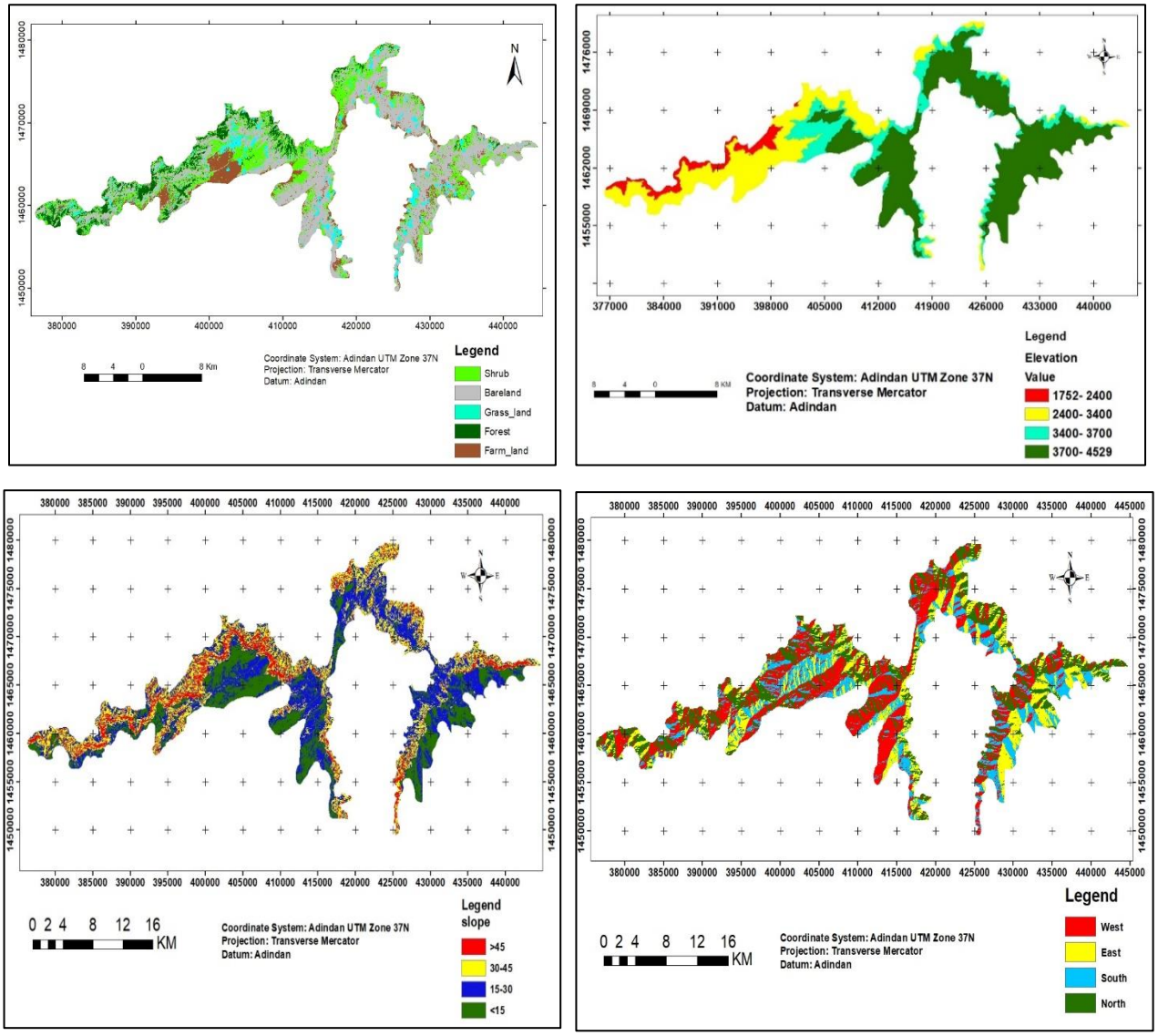


**Fig. 5.** Input factor maps of biophysical risk sub model

The following formula was used to create the biophysical risk sub-model:

BM=W1*LULC+W2*Elevation +W3*Slope +W4*Aspect (6)

BM stands for biophysical risk sub-models, LULC is for land use land cover, and W stands for weight. According to Burgess (2011) and Kant et al (2012) land cover type had a greater significance value compared to other factors (Elevation, Slope and Aspect). the studies of Tafesse (2016); (Burgess, 2011) showed that elevation and slope were found to be more significant over aspect and the two factors( elevation and slope) were given equal weights. The weights of the relative importance of these factors was assigned by using pairwise comparison matrix method through IDRISI SELVA 17.0 software (Table 9).

**Table 9.** Pairwise comparison matrix and result factor weights

| Factors | LULC | Elevation | Slope | aspect | Weights |
|---|---|---|---|---|---|
| LULC | 1 | | | | 0.42 |
| Elevation | 1/2 | 1 | | | 0.23 |
| Slope | 1/2 | 1 | 1 | | 0.23 |
| aspect | 1/3 | 1/2 | 1/2 | 1 | 0.12 |
| Consistency Ratio (CR)= 0.00 | | | | | |

According to Burgess (2011), a consistency ratio (CR) value lower than 0.1 is accepted. In the current study, the consistency ratio to create a biophysical risk sub model is 0.00. Since the value is less than 0.1, it is acceptable (Table 9). By using the weights determined by pairwise comparison, biophysical risk sub model was calculated using the following equation:

BM =0.42* LULC + 0.23* Elevation +0.23*Slope + 0.12*Aspect (7)

#### 3.3.3.2. Formation of Ignition Sub model

The ignition sub model is related to human activities like careless use/disposal of cigarettes, fireworks, and campfires (Orozco, 2008). The firebrand is defined as human residential and agricultural areas where slash and burn farming is practiced. The risk of igniting is increased, as the fuel gets closer to the firebrand. The ignition risk model was constructed by applying proximity analysis to the distance from the firebrands' map (Table 10 and Fig.6).

**Table 10.** Ranking for forest fire susceptibility in ignition sub model.

| **Variable factors** | **Sub class ranges** | **Rank** | **Fire sensitivity** |
|---|---|---|---|
| Distance from Settlement (m) | < 1000 | 1 | Very high risk |
| | 1000-2000 | 2 | High risk |
| | 2000-3000 | 3 | Moderate risk |
| | >3000 | 4 | Low risk |
| Distance from Road (m) | <1000 | 1 | Very high risk |
| | 1000-2000 | 2 | High risk |
| | 2000-3000 | 3 | Moderate risk |
| | >3000 | 4 | Low risk |

**Source:** (Suryabhagavan et al., 2016) ; (Genanaw, 2008)

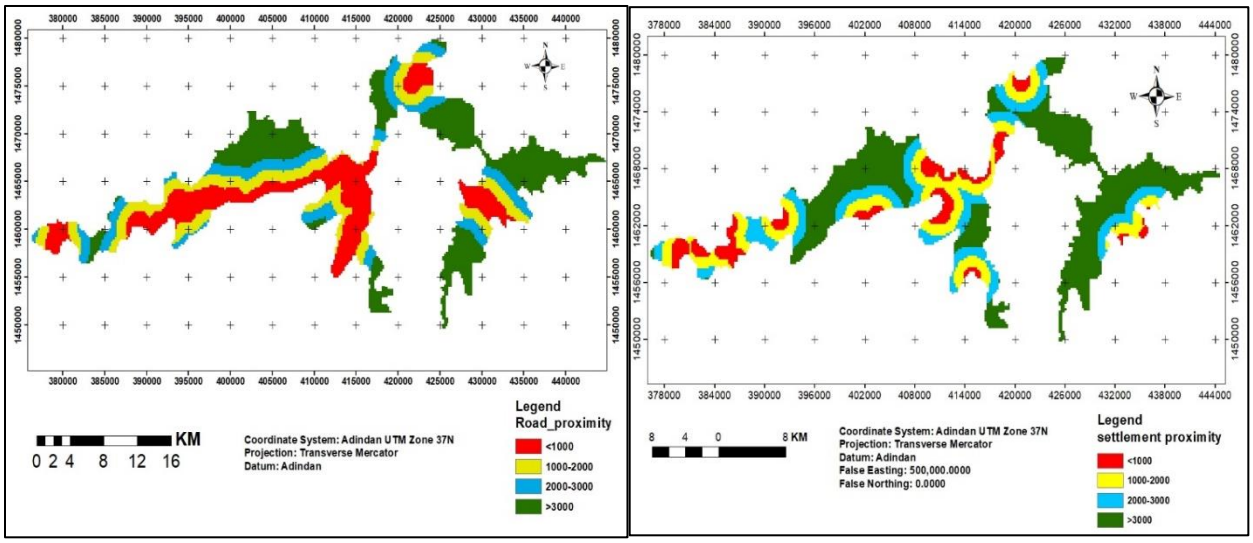


**Fig. 6.** Input factor maps for ignition risk sub model

According to Tafesse (2016), components in the ignition sub-model were given identical weight ratings in the current investigation. The Ignition Sub-model had been multiplied by their respective weights of distance to settlement and road. Finally, create a fire risk zone map for the research region using the Ignition Sub-model. The research utilized the following equation to generate the Ignition sub-model by giving equal weights:

$$IM=0.5(DS) +0.5(DR) \quad (8)$$

Where IM stands for Ignition Sub-model, DS stands for Distance from Settlement; DR is for Distance from Road.

#### 3.3.3.3. Formation of Final Forest Fire Risk Model

The biophysical risk, ignition risk model, and normalized burn ratio map were utilized as inputs to create the final forest fire risk vulnerability. According to (Suryabhagavan et al., 2016), (Genanaw, 2008) and (Tafesse, 2016) forest fire factors that are included in biophysical sub model (LULC , slope, aspect and elevation) have been given higher weights than that of included in ignition sub model (distance from settlements and roads).The weighted overlay analysis approach is used with ArcGIS spatial analyst. Each dataset raster model has a value of 1 to 4. The Pair wise comparison matrix method was used to overcome personal bias in giving weight to each data set. Therefore, the final output of the forest fire risk vulnerability map was generated by multiplying each factor by their corresponding weights acquired from the paired wise

comparison. Biophysical risk to biophysical risk, dNBR to biophysical risk, dNBR to dNBR, ignition to biophysical risk, ignition to dNBR, and ignition to ignition are all compared in Pairwise comparison matrix.

**Table 11.** Pairwise comparison to determine eigenvector weights

| Factors | Biophysical | dNBR | Ignition | Weights |
|---|---|---|---|---|
| Biophysical | 1 | | | 0.41 |
| dNBR | 0.75 | 1 | | 0.24 |
| Ignition | 0.65 | 0.6 | 1 | 0.35 |
| Consistency Ratio (CR)= 0.01 | | | | |

At the end of the process Eigenvector weights: for biophysical risk, normalized burn ratio (NBR) and ignition is 0.41, 0.35 and 0.24 respectively (Table 11). The following equation is crucial in determining the final forest fire risk zone.

FFRZ =0.41* BM +0.24* IM + 0.35*dNBR (9)

Where, FFRZ = Forest fire risk zone, BM= biophysical risk sub-models, IM = Ignition Sub-model and dNBR = Difference Normalized Burn Ratio.

#### 3.3.3.4. Model Validation

According to Burgress (2011), validation is a critical step in the process of building any model. It is vital to compare the model's results to the real world in order to determine the correctness of its performance. In the current study, by obtaining (x, y) coordinate points from Google Earth image of the previously burnt area through displaying burnt date, the model was validated. By overlaying these points with the final forest fire risk model.

### 3.3.3.5. Methodological Flow Chart of the Study

To execute the intended objectives, different data was collected from various sources. The data was created from multi- temporal satellite images. For accuracy assessment and model validation coordinate points were generated from Google earth pro images. In addition, the shape files of road and settlements were employed. To accomplish this study the following flowchart was applicable (Fig.7)

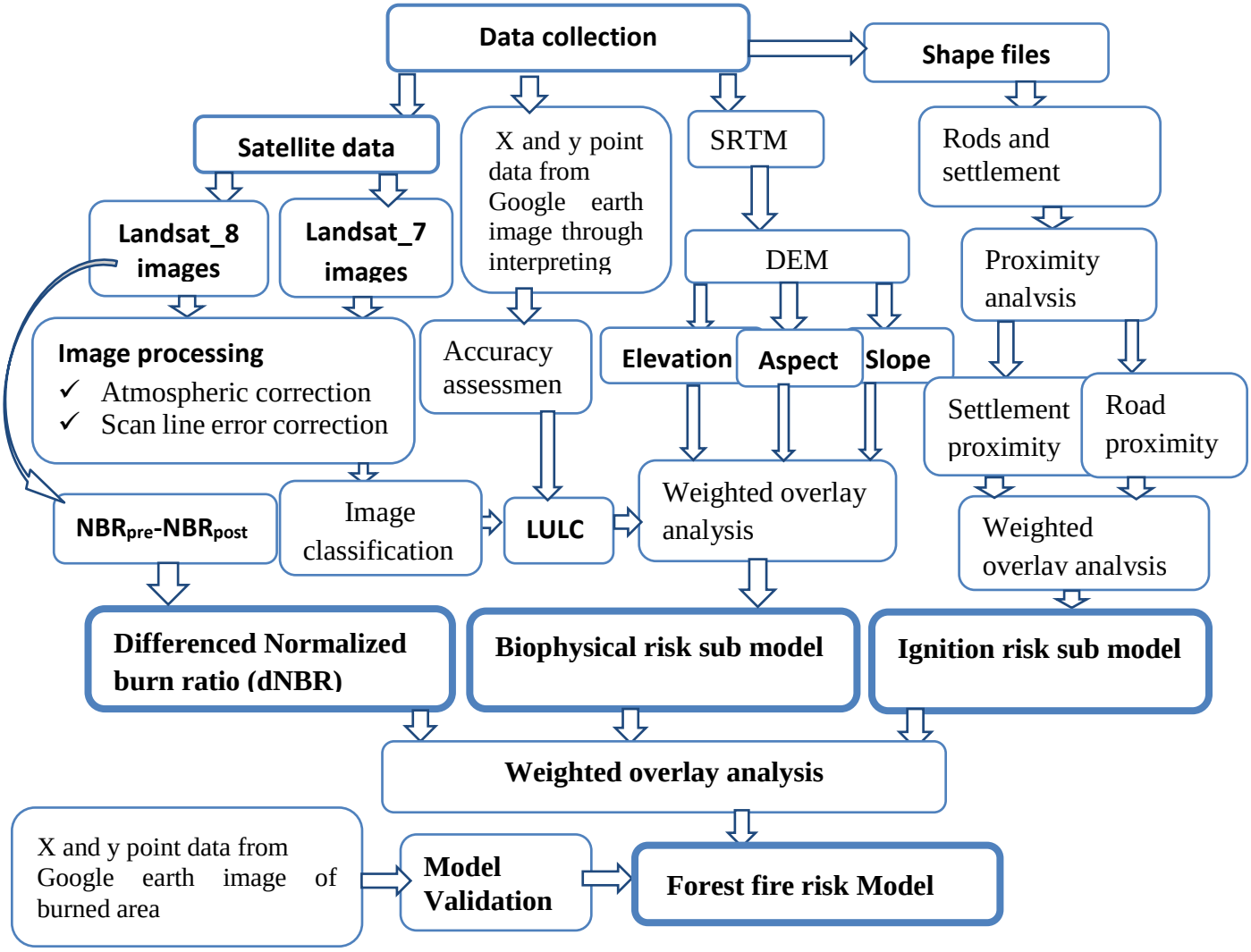


**Fig. 7.** The overall Methodological flow-chart of the study

# CHAPTER FOUR

# 4. RESULTS

This chapter presents the results and discussion of the previous forest fire extents, land use/land cover change dynamics, and finally, the map of fire risk and forecast of what future forest fire risk looks like in SMNP.

## 4.1. Fire Loss Extent Mapping Using dNBR

In the current study area, the value of the calculated difference of normalized burn ratio ranges from -0.63 to 0.75 (Fig.14). As the dNBR map indicated, the dark color represents the low value of dNBR and it had low level of burn severity. On the other hand, the light grey color showed high value, which had high level of burn severity.

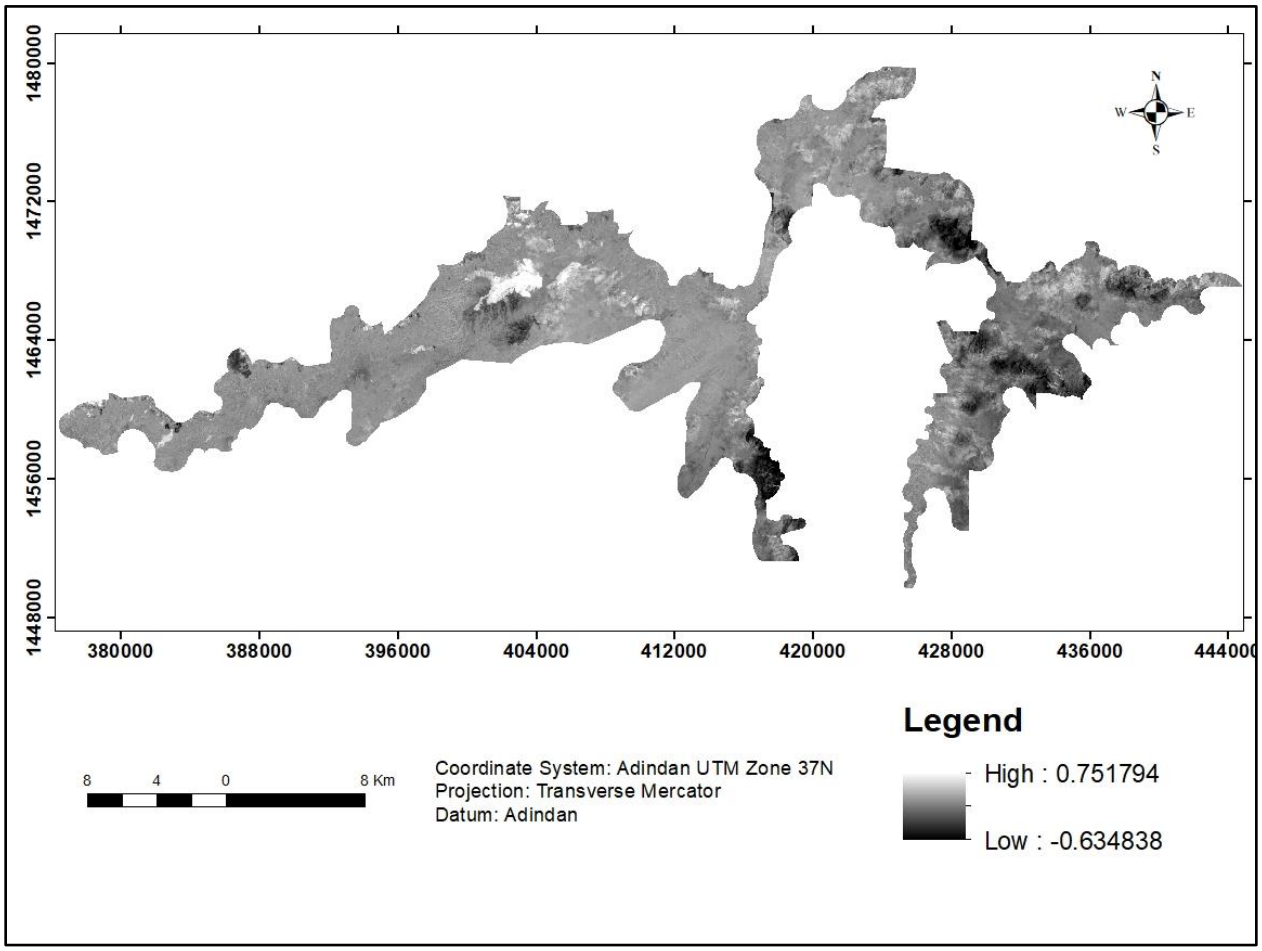


**Fig. 8**. Difference normalized burn ratio (dNBR) map

The fire extent of the study area was reclassified into four burn severity levels; these are high, moderate and low unburned. The output of this study showed that the extent of burn severity as high, moderate and low levels of fire extents covered 10.17%, 42.61%, 38.03% and 9.18% respectively. From the total of the study area, high (red color) and moderate burn severity (yellow color) covered 52.79% (Table 12 and Fig.9).

**Table 12.** Fire extent damaged level and covered area of SMNP

| Value of dNBR ranges | Burn severity levels | Area(ha) | Area (%) |
|---|---|---|---|
| 0.44 - 0.79 | High | 4191.48 | 10.17 |
| 0.27- 0.44 | Moderate | 17557.18 | 42.61 |
| 0.10 - 0.27 | Low | 15668.72 | 38.03 |
| -0.10 – 0.10 | Unburned | 3782.62 | 9.18 |
| Total | | 41200 | 100 |

**Source:** Calculated from the re-classed difference normalized burn ratio (dNBR)

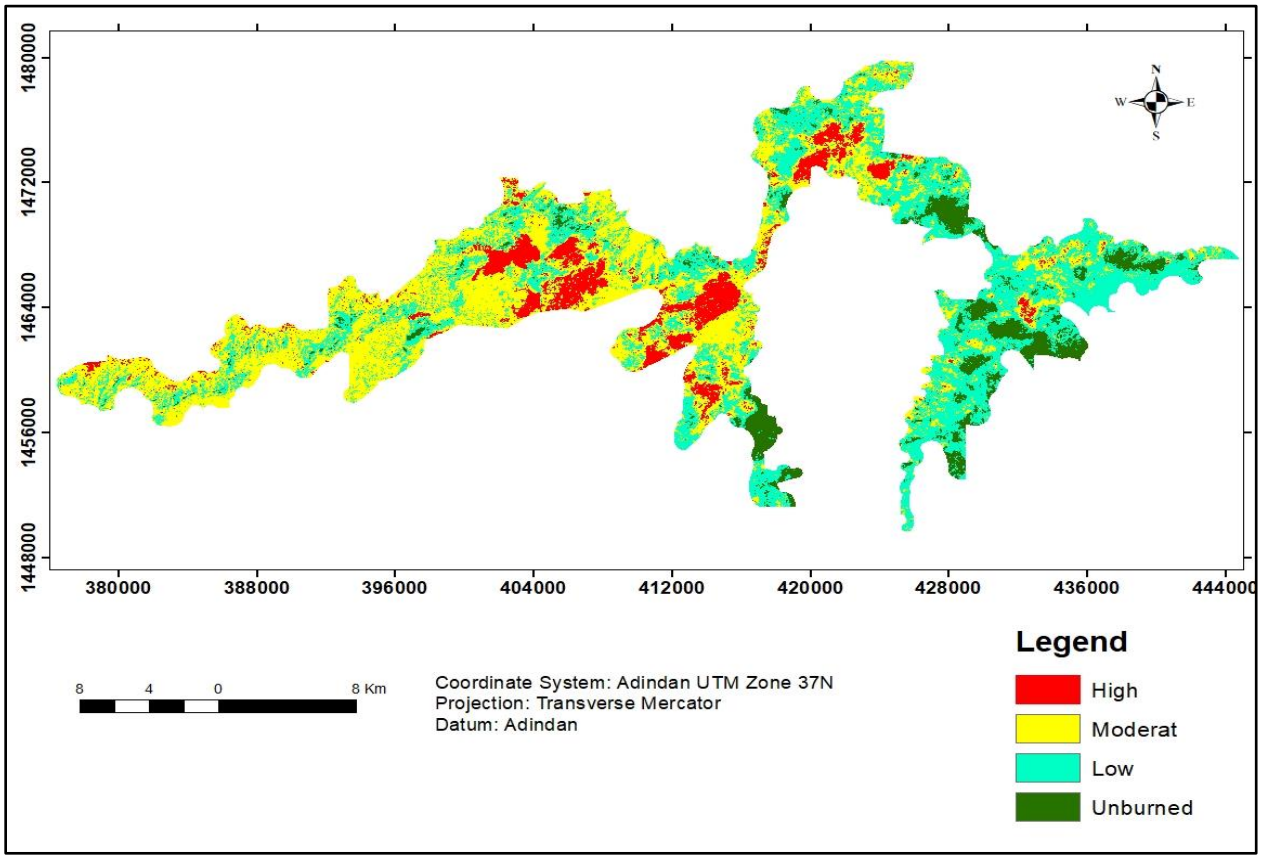


**Fig. 9.** Reclassified difference normalized burn ratio (dNBR) map

## 4.2. Land Use Land Cover Change Dynamics

In the study area, the temporal dynamics of various land use/land cover categories have been analyzed between 2010, 2015 and 2019 to determine the level of change. For this purpose, satellite images of 2010, 2015 and 2019 have been used. The dominant LULC types extracted from the three images were shrubs, grassland, forest, farmland & settlements, and bare land. The land cover maps of the park for the three reference years showed that the LULC patterns of the study area have significant variations over the entire study period. The two years (2010 and 2015), LULC classes showed almost similar pattern but the third one (2019) indicated differences compared to the first LULC classes, some of the LULC classes converted to bare land (Fig.13).

### 4.2.1. Land use/land cover of 2010

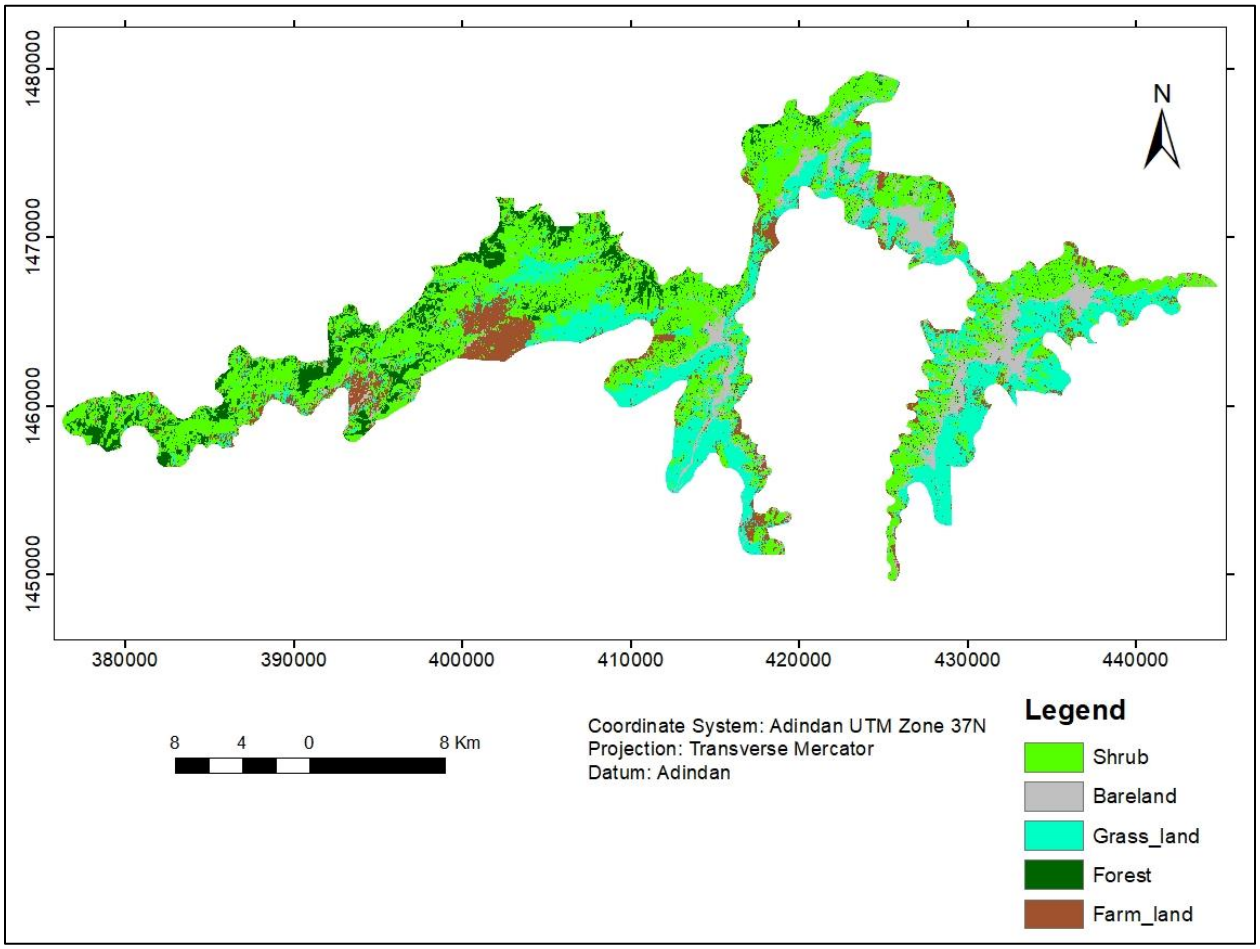


**Fig. 10.** Land use/land cover map of SMNP 2010

The major land use/land cover classes of 2010 include shrubs, grassland, forest, farmland & settlements, and bare land & rocks. As indicated in (Fig 10), the greatest share of land use/land cover among all classes is shrubs, which cover an area of 18954.71ha and contribute 46.01% of the total area. Grassland, and farmland & settlement cover an area of 10166.11 ha (24.68%) and 4313.18 ha (10.47%) respectively. Whereas the coverage of bare land and forest was 4061.62ha (9.86%), 3704.37ha (8.99%) of the total area of the park. This showed that shrubs and grassland covered 70.69% of the total area of the park and farmland & settlement, bare land and forest covered the remaining 29.31% (Fig 10 and Table 13).

### 4.2.2. Land use/land cover of 2015

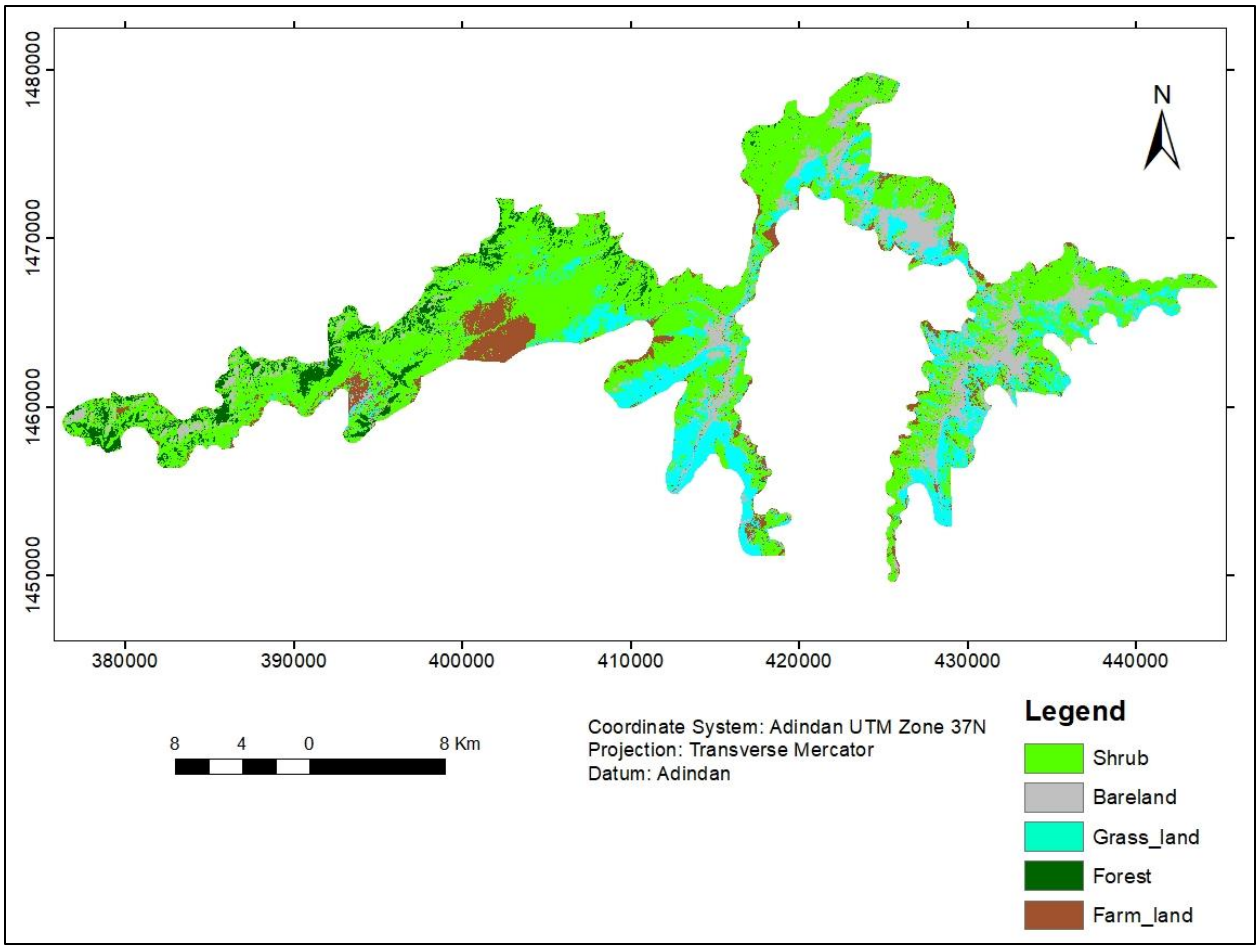


**Fig. 11**. Land use/land cover map of SMNP 2015

Whereas in the case of 2015, the major land use/land cover classes were similar to those of 2010. As indicated in Fig. 11 and table 13, the greatest area of land use/land cover of all classes was

Shrubs land, which covers an area of 18927.08ha (45.94%). Grassland, and farmland & settlement cover an area of 10186.98ha (24.73%) and 4320.52ha (10.49%) respectively. The least area coverage was bare land & rocks and forest, which have only 4052.40 ha (9.84%) and 3713.02 ha (9.01%) respectively of the total area of the park.

### 4.2.3. Land use/land cover of 2019

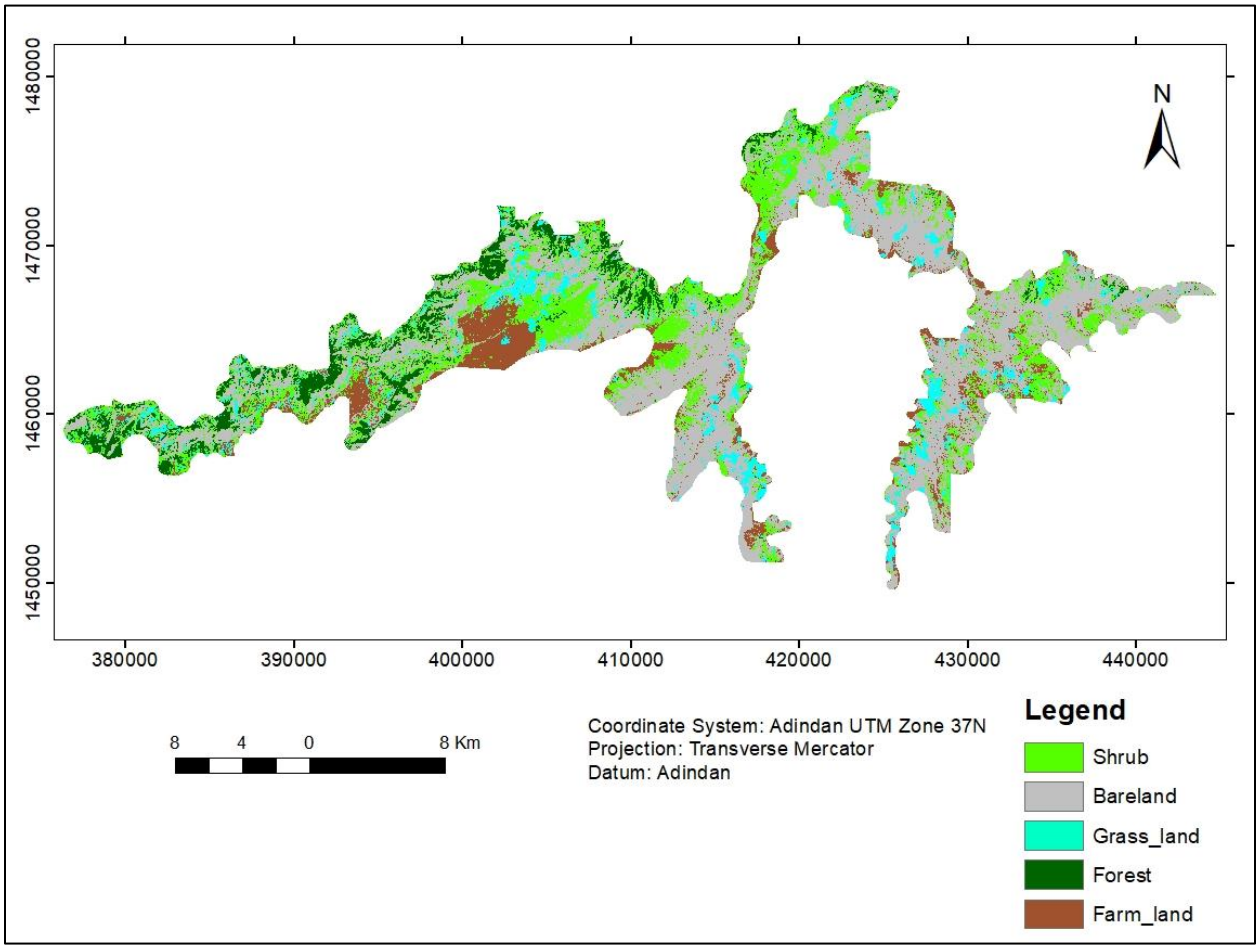


**Fig. 12.** Land use/land cover map of SMNP 2019

During 2019, the major land use/land cover classes included are identical to those in 2010 and 2015; however, all the land use classes have different area coverage from the previous time. The greatest portion of land use/land cover from all classes was bare land and rocks, which covered 19022.15 ha (46.17%). Shrubs, grassland and farmland & settlements cover 9832.75ha (23.87%), 4348.41ha (10.55%), 4332.4ha and (10.52%) respectively. The least area was covered by forest, which is 3664.62ha (8.89%) of the park's total area (Fig 12 and Table 13).

**Table 13 .** LULC area coverage of the study between 2010 and 2019

| LULC classes | 2010 area coverage | | 2015 area coverage | | 2019 area coverage | |
|---|---|---|---|---|---|---|
| | ha | % | ha | % | ha | % |
| Shrubs | 18954.71 | 46.01 | 18927.08 | 45.94 | 9832.75 | 23.87 |
| Forest | 3704.37 | 8.99 | 3713.02 | 9.01 | 3664.62 | 8.89 |
| Grassland | 10166.11 | 24.68 | 10186.98 | 24.73 | 4348.41 | 10.55 |
| Farmland and settlement | 4313.18 | 10.47 | 4320.52 | 10.49 | 4332.41 | 10.52 |
| Bare land and rocks | 4061.62 | 9.86 | 4052.40 | 9.84 | 19022.15 | 46.17 |
| Total | 41200 | 100.00 | 41200.00 | 100.0 | 41200.34 | 100.00 |

**Source:** Computed from Satellite Image of LULC of 2010, 2015 and 2019.

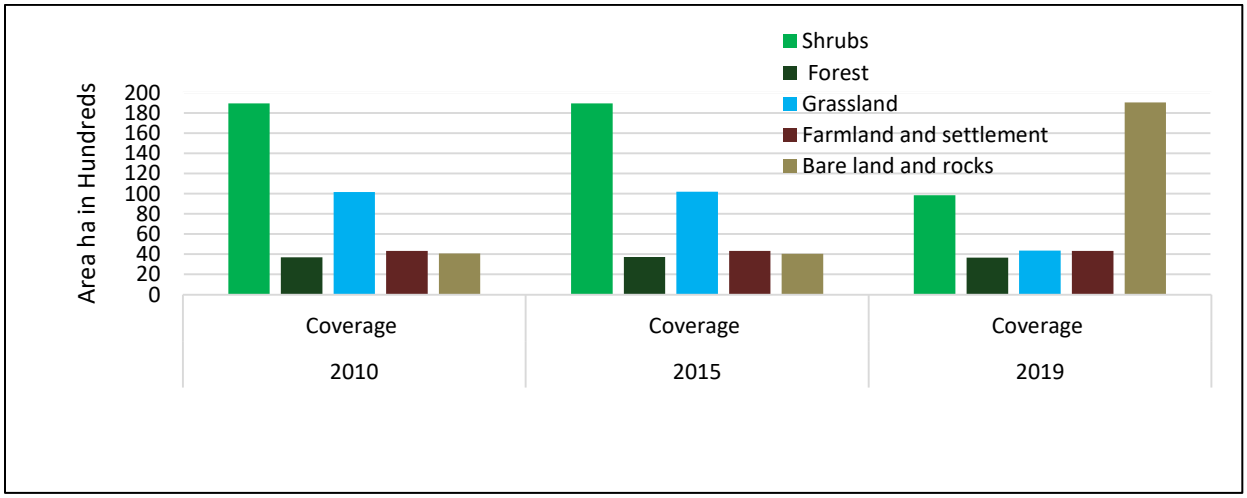


**Fig. 13.** LULC patterns of the study area between 2010, 2015 and 2019

## 4.3. Rate of LULC Change between the Year 2010-2015 and 2015 -2019

The land use land cover percentage, area coverage and rate of change for each land category for all the different years are calculated from table 13. The rate of change-calculated result is shown in the following table.

**Table 14 .** Summary Statistics of LULC of SMNP between 2010, 2015 and 2019

| Covered classes | Rate of change | |
|---|---|---|
| | 2010 and 2015(ha) | 2015 and 2019(ha) |
| Shrubs | -5.53 | -2273.61 |
| Forest | 1.73 | -12.13 |
| Grassland | 4.17 | -1459.67 |
| Farmland & settlement | 1.47 | 2.97 |
| Bare land and rocks | -1.84 | 3742.43 |
| Total | 0.00 | 0.00 |

Source: computed from the classified Landsat 2010 and 2015 and 2019 imageries

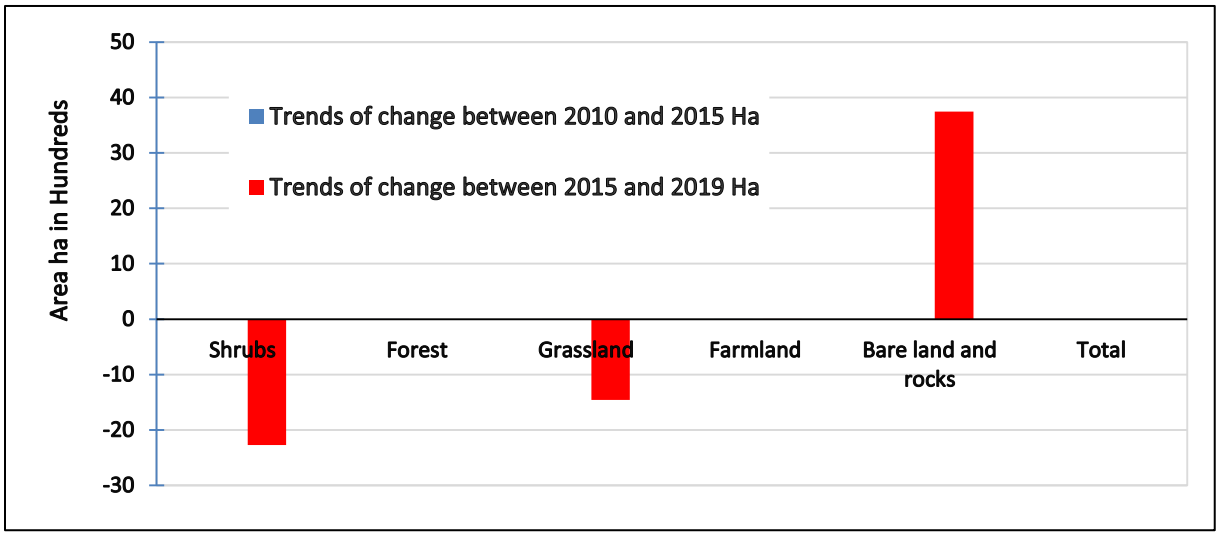


**Fig. 14**. Trends of LULC change between 2010-2015 and 2015-2019

As the result of the study indicated, the trend of LULC between 2010 and 2015, no exaggerated change was observed. In this period, forest, grassland and farmland & settlement increased at the rates of 1.73 ha, 4.17 ha and 1.47 ha respectively per annum in a 5 year period. In contrast, in a similar period, shrubs and bare land decreased at a rate of 5.53 ha and 1.84 ha per year, respectively for a consecutive 5 years (Table 14 and Fig.14). In contrast, between 2015 and 2019, there was a dynamic change in shrubs (-2273.61ha), grasslands (-1459.67ha), forests (-12.13ha), and bare lands (3742.43ha) per year. Shrubs, grassland and forests negatively changed, which leads to the increment of bare lands & rocks as well as farmland & settlement. In the study area, there was an

uncontrolled fire extent in 2019 and caused the loss of grassland, shrubs and forests. This fire extent resulted in an increase of bare land.

## 4.4. Accuracy Assessment

The result of the three-year accuracy assessment is presented in the following tables.

**Table 15.** Classification accuracy assessment and kappa statistics report for 2010

| Class Name | Reference Totals | Classified Totals | Number Correct | Producers Accuracy | Users Accuracy | Kappa |
|---|---|---|---|---|---|---|
| Farmland & settlement | 50 | 50 | 47 | 94.00% | 94.00% | 0.92 |
| Bare land rocks | 50 | 48 | 47 | 94.00% | 97.92% | 0.97 |
| Grass land | 48 | 48 | 43 | 89.58% | 89.58% | 0.89 |
| Shrub | 50 | 58 | 50 | 100.00% | 86.21% | 0.83 |
| Forest | 53 | 46 | 46 | 86.79% | 100.00% | 1.00 |
| Totals | 251 | 251 | 233 | | | |
| Overall Classification Accuracy = | | 92.83% | | Overall Kappa Statistics = 0.91 | | |

**Table 16**. Classification accuracy assessment and kappa statistics report for 2015

| Class Name | Reference Totals | Classified Totals | Number Correct | Producers Accuracy | Users Accuracy | Kappa |
|---|---|---|---|---|---|---|
| Shrubs | 47 | 46 | 43 | 91.49% | 93.48% | 0.92 |
| Grass land | 51 | 55 | 48 | 94.12% | 87.27% | 0.84 |
| Bare land and rocks | 51 | 52 | 48 | 94.12% | 92.31% | 0.90 |
| Farmland & settlement | 50 | 49 | 46 | 92.00% | 93.88% | 0.92 |
| Forest | 54 | 52 | 51 | 94.44% | 98.08% | 0.98 |
| Totals | 254 | 254 | 236 | | | |
| Overall Classification Accuracy = | | 92.91% | | Overall Kappa Statistics = 0.91 | | |

**Table 17.** Classification accuracy assessment and kappa statistics report for 2019

| Class Name | Reference Totals | Classified Totals | Number Correct | Producers Accuracy | Users Accuracy | Kappa |
|---|---|---|---|---|---|---|
| Farmland and settlement | 50 | 51 | 50 | 100.00% | 98.04% | 0.98 |
| Shrubs | 52 | 66 | 44 | 84.62% | 66.67% | 0.58 |
| Bare land and rocks | 52 | 51 | 49 | 94.23% | 96.08% | 0.95 |
| Grassland | 50 | 47 | 43 | 86.00% | 91.49% | 0.89 |
| Forest | 53 | 42 | 37 | 69.81% | 88.10% | 0.85 |
| Totals | 257 | 257 | 223 | | | |
| Overall Classification Accuracy = | | 86.77% | | Overall Kappa Statistics = 0.8346 | | |

Based on accuracy assessment analysis of LULC maps for the three years 2010, 2015 and 2019, the overall classification accuracy was 93.15%, 92.91% and 86.77% and the kappa coefficients are 0.91, 0.91 and 0.83 respectively for the three consecutive years (Tables 15, 16 and 17).

## 4.5. Development of Forest Fire Risk model in SMNP

In the current study to map and forecast the future forest fire risk, the biophysical risk and ignition risk sub models were engaged. To produce these two models data set preparation is a prerequisite activity to identify forest fire risk areas. After the preparation of the two-mentioned models, the final forest fire risk model was produced by overlaying with the NBR map.

### 4.5.1. Formation of biophysical risk sub model

The biophysical risk sub-model is the most important model and it includes reclassified raster layers that are LULC, slope, aspect and elevation. As presented in the table 18, fire risk levels are grouped into four risk zone classes. Accordingly, the very high fire risk area (red color) covers 34.76km$^2$ (8.44%) of the total area , 272.93km$^2$ (66.25%) is a high risk (the yellow color) which covers the largest area, 48.82km$^2$ (11.85%) is a moderate risk (blue color) and 55.49km$^2$ (13.47%) of the study area shows a low risk zone (Table 16 Fig.15).

**Table 18.** Area and percentage of fire risk zone in biophysical risk sub model

| risk zone | Fire risk | Area(km$^2$) | Area (%) |
|---|---|---|---|
| 1 | Very high risk | 34.76 | 8.44 |
| 2 | High risk | 272.93 | 66.25 |
| 3 | Moderate risk | 48.82 | 11.85 |
| 4 | Low risk | 55.49 | 13.47 |
| Total | | 412 | 100 |

Source: Calculated from overlay analysis in ArcGIS, attributes of Biophysical risk sub model

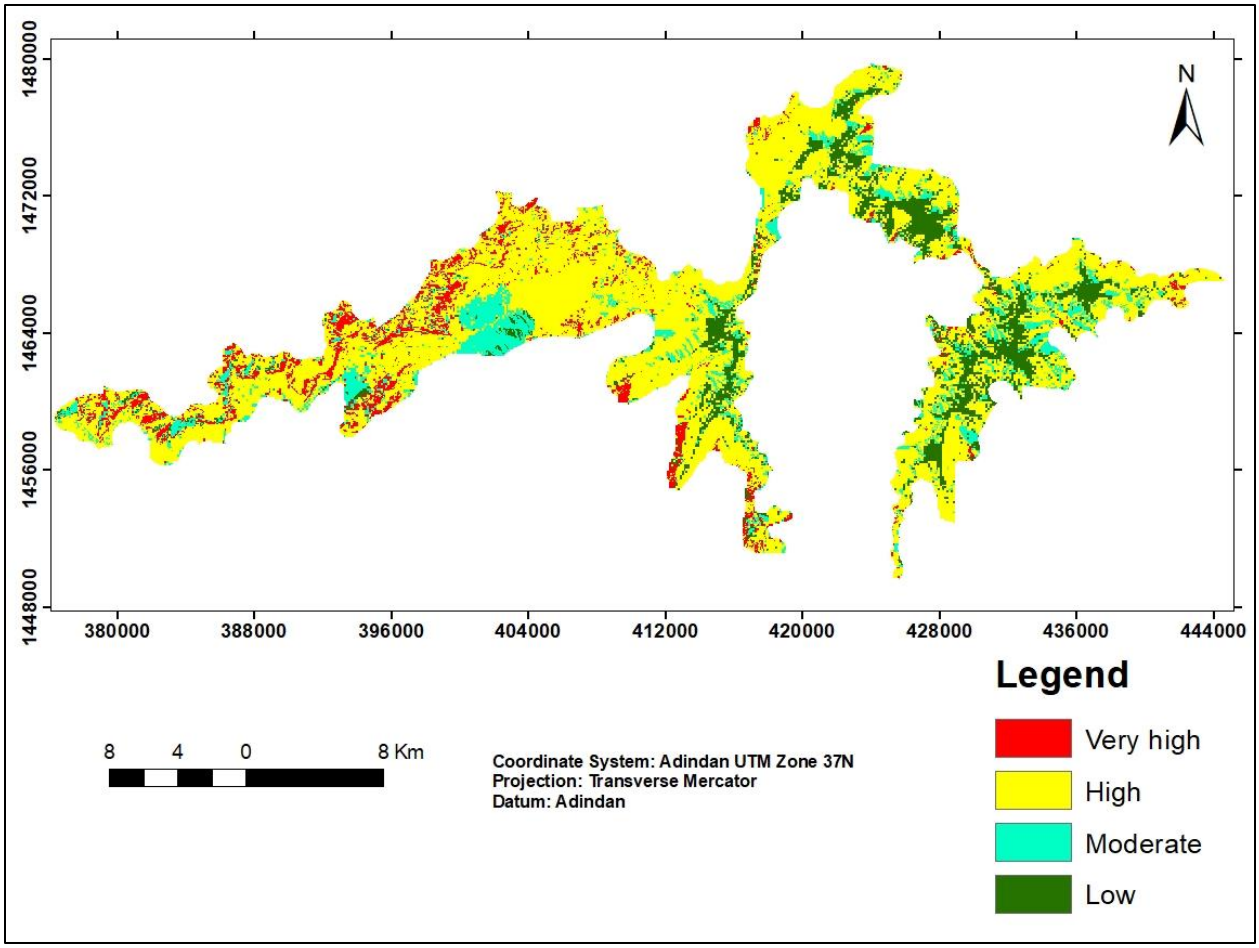


**Fig. 15.** Biophysical risk sub model map of SMNP

### 4.5.2. Producing ignition sub model

As described in chapter three of the current study, the ignition sub model includes proximity to settlements and roads. These two factors have their own influence weights in forecasting the forest fire risk zone of the study area. By using ArcGIS 10.4, proximity analysis was performed on road network and distance from settlements by creating buffers according to the specifications mentioned in (Table 15). As the area is very close to the settlements and the roads, the degree of fire risk is very high. As indicated in the result of the ignition sub model, from the total area of 412km² about 95.33 $km^2$ (23.14%) indicates a very high degree of fire risk zone (red color) which is closer to the roads and settlements. The area which is represented by yellow color (high degree of fire risk) covered 62.32$km^2$ (15.13%) of the total study area, 82.71$km^2$ (20.08%) moderate risk and 171.64$km^2$ (41.66%) shows a low degree of fire risk zone. (Table 19 and Fig 16).

**Table 19**. Area and percentage of fire risk zone in ignition sub model

| risk zone | fire risk | Area($km^2$) | Area (%) |
|---|---|---|---|
| 1 | very high risk | 95.33 | 23.14 |
| 2 | High risk | 62.32 | 15.13 |
| 3 | Moderate risk | 82.71 | 20.08 |
| 4 | Low risk | 171.64 | 41.66 |
| Total | | 412.00 | 100.00 |

Source: Calculated from proximity analysis in ArcGIS attributes of ignition sub model

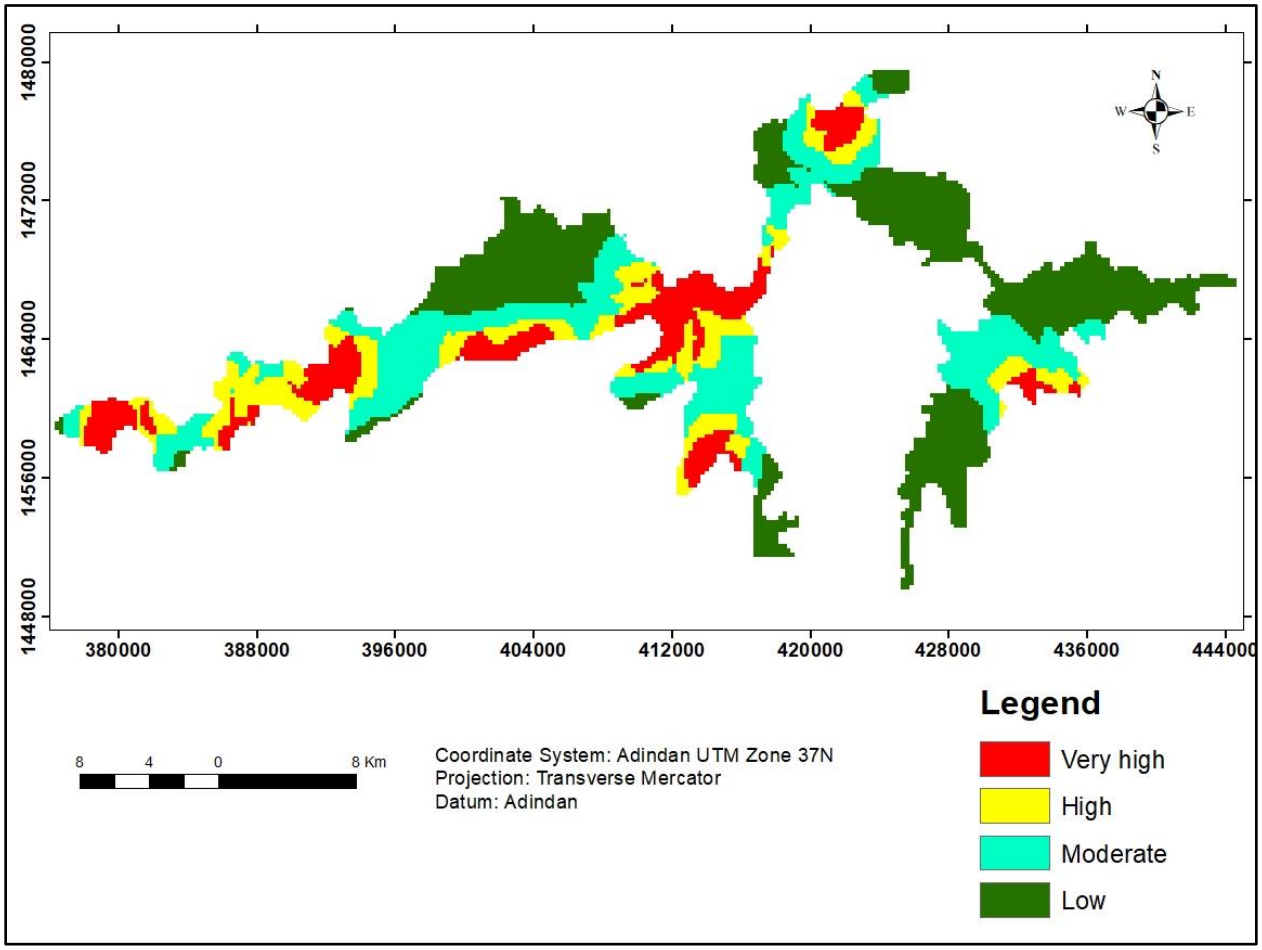


**Fig. 16**. Ignition risk sub model map of SMNP

### 4.5.3. Forest fire risk model

Biophysical risk submodel, ignition risk submodel, and difference normalized burn ratio (dNBR) map dataset layers were used to create a forest fire risk model. As a result, the final forest fire risk model showed that 67.86 $km^2$ (16.47%) of the area is very high fire risk zones (red color), high fire risk zone (yellow color) constitutes about 78.53 $km^2$ (19.06%) and moderate fire risk zone(blue color) covers 191.82 $km^2$ (46.56%). The rest 73.79 $km^2$ (17.91%) of the park categorized under Low-risk zone (green color). Overall, the final forest fire risk model map has indicated that there are considerable regions that fall into the very high and high fire risk zones, covering about 146.39 $km^2$ (35.53%) (Table and Fig.17). As indicated in the map, most of the western part of the study area is under very high and high level of fire risk (Fig.17).

**Table 20**. Area coverage of the final forest fire risk model result

| Risk zones | Fire risk | Area ($km^2$) | Area (%) |
|---|---|---|---|
| 1 | Very high | 67.86 | 16.47 |
| 2 | High | 78.53 | 19.06 |
| 3 | Moderate | 191.82 | 46.56 |
| 4 | Low | 73.79 | 17.91 |
| Total | | 412.00 | 100.00 |

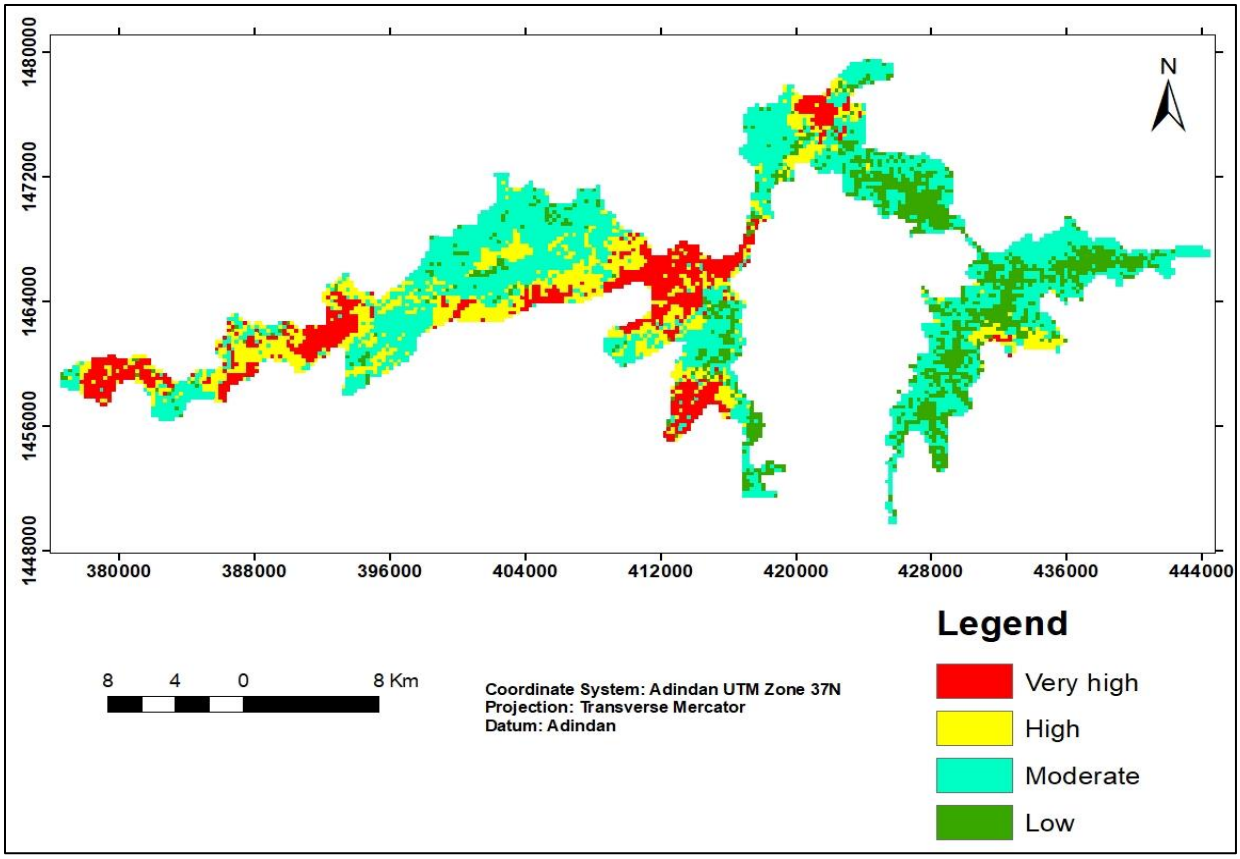


**Fig. 17**. Forest fire risk map

### 4.5.4. Model Validation

To validate the study's findings, 129 sample points were employed. From 129 sample points, 86.05% of the total fall within the first two-forest fire danger zone's very high and high-risk levels. Consequently, most of the points were overlapping with those areas under very high and high fire risk zones of the final risk model map. Therefore, it is possible to conclude that the model performance is very good and illustrative (Table 21).

**Table 21.** Distribution of validation points

| No | Degree of fire risk | Validation points | Area (%) |
|---|---|---|---|
| 1 | Very high | 38 | 29.46 |
| 2 | High | 72 | 56.59 |
| 3 | Moderate | 13 | 9.30 |
| 4 | Low | 6 | 4.65 |
| Total | | 129 | 100.00 |

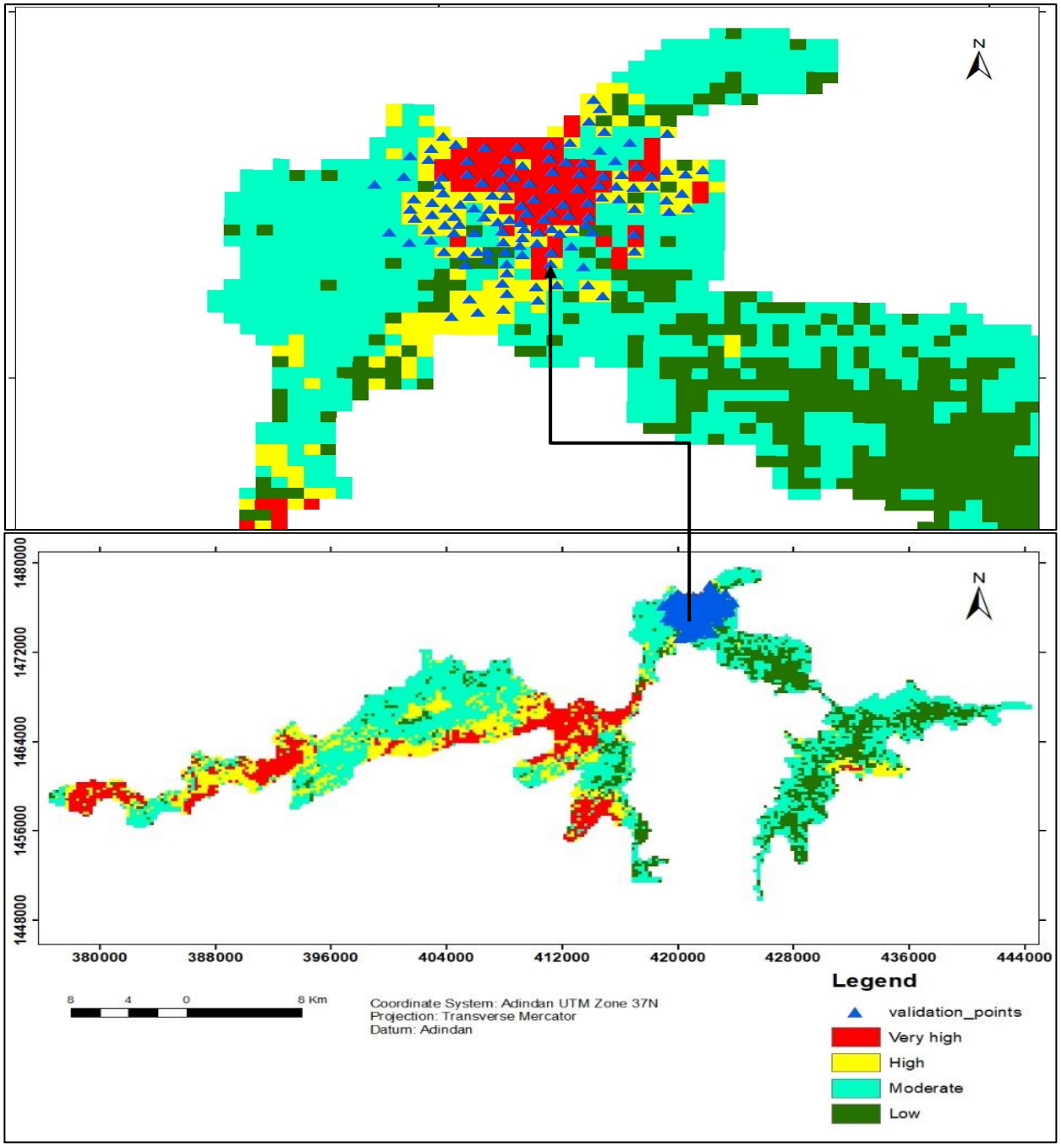


**Fig. 18.** The final forest fire risk Model validated map

# CHAPTER FIVE

# 5. DISCUSSION

## 5.1. Fire loss extent mapping

The difference of pre and post fire normalized burn ratios (dNBR) was used to determine fire severity, as described in Chapter four of this study. Different researchers in different study area assessed the fire severity. Some of them are; Lentile et al., (2006);; (Escuin et al., 2008); Fang & Yang, (2014) ; Melchiorre & Boschetti, (2018); Rodriguez (2021).

The difference normalized burn ratio (dNBR) was used to assess burn severity. Therefore, the result of this study is in line with the previous work of the above-mentioned authors. For example Lentile et al., (2006) stated that by using remotely sensed data the difference Normalized Burn Ratio between pre and post-fire images (dNBR) calculated and widely used to infer fire severity. The pixels with the lowest dNBR values correspond to the unburned class, the intermediate values to the moderate class and the pixels with the highest values of dNBR correspond to the extreme class (Escuin et al., 2008). Rodriguez (2021) argues that, the difference of the two-raster maps (pre and post fire) creates a scale where positive values indicate a higher level of damage.

The result showed that a significant area is under high fire severity. Therefore, this study helps to decrease forest fire risk in the future and to monitor post fire management by identifying the hotspot area.

## 5.2. Assessing LULC changes

The change of LULC assessed by identifying the dominant LULC classes (forest, shrub, grassland, farmlands and bare land). Based on accuracy assessment analysis of LULC maps for the three years 2010, 2015 and 2019, the overall classification accuracy and the kappa coefficients are within the acceptable range which are greater than 0.80. According to Landisand Koch (1977), Congalton and Green (2009) a computed Kappa value greater than 0.80 indicates a strong (almost perfect) agreement.

Between 2015 and 2019; Shrubs, grassland and forests negatively changed, which leads to the increment of bare lands & rocks as well as farmland & settlement. In the study area, there was

an uncontrolled fire extent in 2019 and caused the loss of grassland, shrubs and forests. This fire extent resulted in an increase of bare land and rocks.

According to Masresha (2019), from the period 1994 to 2017, grassland and bare land showed a positive rate of change, but farmland and forest indicated a negative. During crop growing period, moorlands of the SMNP are land of common use (to graze livestock). Overgrazing may result change in floristic composition, biodiversity decline, affect soil structure (soil compaction), and even it can totally remove the vegetation. In the current study, from 2015 to 2019, farmland and bare land indicated a positive rate of change, but the rate of bare land was highly increased. On the contrary, grassland showed a negative rate of change because an unexpected and uncontrolled fire extent occurred in the study area and damaged large areas of grassland and shrubs.

Therefore, by understanding the current condition of the study area the result helps stakeholders to develop conservation strategies for future sustainable land use strategies.

## 5.3. Modelling forest fire risk zone

In the current study, GIS and Remote Sensing is applicable for Modeling and mapping a fire risk by using different parameters for analyzing their effects in forest fire in different sub models. In this study, the biophysical risk, ignition risk and the integrated forest fire risk model were developed using different risk factors.

The biophysical risk sub model was produced based on the properties of LULC type, aspect, slope, and elevation. As the study indicated, the majority of very high and high fire risk areas are located in parts of the study area covered by grassland, shrub land, low elevation, steep slope and west aspect large to least areas respectively. Therefore, this is predictable outcome due to the value assigned to LULC map, (the greatest value was assigned to the grassland area). In the same study, to predict the fire risk area for the future, the researchers in several study areas used these parameters. Some of them are Kant et al. (2012); (Suryabhagavan et al., 2016b); (Tafesse, 2016); stated that in the biophysical sub model, LULC type had a greater significance value compared to other factors (elevation, slope and aspect). Burgess (2011) and Tafesse (2016) argue that elevation and slope were found to be more significant over aspect, Elevation and slope have equal weights.

The study's findings clearly showed that in the ignition sub model, areas with road networks and human settlements have a very high and high fire risk respectively. This is due to the locals' careless and purposeful usage of fire for various purposes. The ignition sub-model was created by giving higher values to locations that are very close to settlements and roads and low values to areas that are very far from both settlement and road accessibility. As a result, lands adjacent to the settlement and the road are in a very high-risk fire zone. The studies by Genanaw (2008), Suryabhagavan et al., (2016b) and Tafesse, (2016) also argue that areas very close to settlements and roads are very high fire risk zones. Ganteaume et al.,( 2013) and Wang et al.,(2018) claimed that the settlements and agricultural areas where slash and burn farming practices occur were recognized as the hotspots. In addition (Suryabhagavan et al., 2016) argue that in the road networks, Human and vehicular movement, as well as activity on tracks, create chances for both accidental and intentional fires.

In the current study, the final forest fire risk model was produced by overlying the biophysical risk sub model, differenced normalized burn ratio (dNBR), and the ignition risk sub model. In general, the result showed that, the western part of the park is very high and high-risk area. The forest fire risk model was developed by Tafesse (2016) integrated the biophysical and ignition risk sub models and giving the biophysical sub model more weight than the ignition sub model and Suryabhagavan et al. (2016) also used the factors of these two models. The LULC, aspect, slope, and elevation risk zone maps are combined to create the biophysical risk sub model, which has been assigned the first maximum weightage in the final forest fire risk model. The most of very high and high fire risk zones are located in grass and shrubby parts of the study area. This is a expectable finding due to the value assigned to the LULC, the greatest value assigned to the grassland area. In a similar study by Suryabhagavan et al. (2016), Tafesse (2016), and Burgress (2011), grassland cover types were associated with very high fire risk. The difference normalized burn ratio (dNBR) index map was given the second influence weight next to the biophysical sub model to produce the final forest fire risk model. Because the pattern of dNBR index map was almost related to the biophysical risk sub model and when validated by using the location points of the previous fire extent areas, the second maximum points are located in areas of very high and high fire risk next to the biophysical sub model.

# CHAPTER SIX

# 6. CONCLUSION AND RECOMMENDATIONS

## 6.1. Conclusion

For mapping forest fire danger extents and modeling fire risk zones, GIS and remote sensing are effective technologies. This study analyzed and discussed the previous forest fire extents, land use /land cover change dynamics and finally mapped fire risk and forecasted fire risk extents in SMNP.

Using Landsat 8 data, the normalized burn ratio (NBR) and the dNBR approach were used to examine prior forest fire extents. The Difference normalized burn ratio (dNBR) index can detect previously burned areas. The majority of fires in the studied area happened between March and May. The data was collected after the fire (on April 13, 2019), taking into account the circumstances. According to the findings, the fire risk levels of high and moderate encompass 4191.48 ha (10.17 %) and 17557.18 ha (42.61 %) of the total area of 41200 ha, respectively. This indicates a large area of the park was damaged by the fire risk the severity of forest fire burns or the effects of fire were assessed using dNBR, and the results were used to inform forest fire management stakeholders.

The results obtained from supervised classified Landsat 7 and 8 imageries from the years 2010, 2015 and 2019 were used to examine the land use /land cover dynamics of the study area under investigation. The dominant LULC types extracted from the three years of images were shrubs, grassland, forest, farmland & settlements, and bare land. Overall classification accuracy of the three years was 93.15%, 92.91% and 86.77% respectively, and the result is within the accepted range of accuracy. Land use /land cover dynamic trends were observed in the study area, to some extent between 2010 and 2015. Accordingly, shrubs and bare land showed negative trends. In addition, in 2015 and 2019 shrubs and grassland showed negative trends indicating the damage of fire on shrubs and grasslands. The study conducted to Provide detail information about LULC dynamics for stakeholders and used for decision-making process to make sustainable environment.

To forecast the future, in the current study, the biophysical risk, the ignition risk sub model and dNBR index were employed. To produce a biophysical risk sub model, the research used LULC, elevation, slope and aspect as parameters. In the ignition risk sub model, proximity analysis was

done by taking distances from the road and settlements as variable factors. The output of the biophysical risk model, very high and high degree of fire risk covers 74.68% and In the same way, the dNBR and ignition risk models cover 52.79 % and 38.27 % of the degree of fire risk, respectively.

Finally, in this paper, the final forest fire risk model was developed using weighted overlay analysis. To perform this model, the biophysical risk sub model, the ignition risk sub model and difference normalized burn ratio (dNBR) was occupied by giving influence weights. This forest fire risk model was validated performed using (x, y) coordinate points obtained from Google Earth by displaying and fixing burnt area. The result indicates 86.05% of the total points overlap under the very high and high-risk levels of the final forest fire risk zone. Consequently, we understand that the final forest fire risk model indicated very good accuracy. From the final model, the research concludes the integration of the three inputs gives the final forest fire risk model map, which indicates significant areas come under very high and high fire risk zone, covering about 35.53% of the total area. Therefore, it is critical to use this forest fire risk model to implement various fire management measures in order to reduce forest fire risks in the research region.

## 6.2. Recommendations

Depending on the research findings of the analysis, the following recommendations are forwarded to overcome the existing problems.

- The result shows that there is a significant area under fire risk, which needs frequent follow up. Therefore, to decrease forest fire risk, the emergency response measures should be undertaken by setting up Forest fire brigade, watchtower, and helicopter water point.
- The result of this study indicates the contribution of spatial analysis for fire risk mapping and modeling. Hence, strongly recommend the use of a forest fire risk model which is produced in this research for SMNP to improve and understand future fire management.
- The researcher advises the adoption of GIS and Remote sensing technology for prevention, monitoring, alertness, readiness, early warning system, early detection, early fire extinguishing and post fire handling
- The investigator also recommends that potential researchers conduct research on the effects of drought on fire-related phenomena.

# References


Adab, H., Kanniah, K. D., & Solaimani, K. (2013). Modeling forest fire risk in the northeast of Iran using remote sensing and GIS techniques. Natural Hazards, 65(3), 1723–1743. https://doi.org/10.1007/s11069-012-0450-8

Alganci, U., Sertel, E., & Ormeci, C. (n.d.). Forest Fire Damage Estimation Using Remote Sensing and GIS. 8.

Asenova, M. (2018). Assessment and Mapping Of Forest Fire Risk Using GIS: A Case Study Of Bulgaria.

Barros, A. M. G., & Pereira, J. M. C. (2014). Wildfire Selectivity for Land Cover Type: Does Size Matter? PLOS ONE, 9(1), e84760. https://doi.org/10.1371/journal.pone.0084760

Berhan, G. (2007). Forest Cover Change and Susceptibility to Forest Degradation Using Remote Sensing and GIS Techniques: A Case of Dendi District, West Central Ethiopia [Masters, Addis Ababa University]. http://thesisbank.jhia.ac.ke/5271/

Burgess, R. (2011). Development of a spatial, dynamic, fuzzy fire risk model for Chitwan District, Nepal [Master's Thesis]. University of Twente.

Centre, U. W. H. (n.d.). A Grazing Pressure Reduction Strategy updated for Simien Mountains National Park. UNESCO World Heritage Centre. Retrieved June 15, 2021, from https://whc.unesco.org/en/news/1482/

Chen, X., Vogelmann, J. E., Rollins, M., Ohlen, D., Key, C. H., Yang, L., Huang, C., & Shi, H. (2011). Detecting post-fire burn severity and vegetation recovery using multitemporal remote sensing spectral indices and field-collected composite burn index data in a ponderosa pine forest. International Journal of Remote Sensing, 32(23), 7905–7927. https://doi.org/10.1080/01431161.2010.524678

Chernet, T., & Consult, E. (2015). A resource base and climate change risk maps for Simien Mountains National Park. PHE-Ethiopia Consortium. Addis Ababa, Ethiopia.

Chuvieco, E., Aguado, I., Salas, J., García, M., Yebra, M., & Oliva, P. (2020). Satellite Remote Sensing Contributions to Wildland Fire Science and Management. Current Forestry Reports, 6(2), 81–96. https://doi.org/10.1007/s40725-020-00116-5

Dangermond, J. (1992). What is a Geographic Information System(GIS)? Geographic Information Systems (GIS) and Mapping—Practices and Standards. https://doi.org/10.1520/STP24180S

De Keukelaere, L., Sterckx, S., Adriaensen, S., Knaeps, E., Reusen, I., Giardino, C., Bresciani, M., Hunter, P., Neil, C., Van der Zande, D., & Vaiciute, D. (2018). Atmospheric correction of

Landsat-8/OLI and Sentinel-2/MSI data using iCOR algorithm: Validation for coastal and inland waters. European Journal of Remote Sensing, 51(1), 525–542. https://doi.org/10.1080/22797254.2018.1457937

Escuin, S., Navarro, R., & Fernández, P. (2008). Fire severity assessment by using NBR (Normalized Burn Ratio) and NDVI (Normalized Difference Vegetation Index) derived from LANDSAT TM/ETM images. International Journal of Remote Sensing, 29(4), 1053–1073. https://doi.org/10.1080/01431160701281072

Fang, L., & Yang, J. (2014). Atmospheric effects on the performance and threshold extrapolation of multi-temporal Landsat derived dNBR for burn severity assessment. International Journal of Applied Earth Observation and Geoinformation, 33, 10–20. https://doi.org/10.1016/j.jag.2014.04.017

Fornacca, D., Ren, G., & Xiao, W. (2018). Evaluating the Best Spectral Indices for the Detection of Burn Scars at Several Post-Fire Dates in a Mountainous Region of Northwest Yunnan, China. Remote Sensing, 10(8), 1196. https://doi.org/10.3390/rs10081196

Ganteaume, A., Camia, A., Jappiot, M., San-Miguel-Ayanz, J., Long-Fournel, M., & Lampin, C. (2013). A Review of the Main Driving Factors of Forest Fire Ignition Over Europe. Environmental Management, 51(3), 651–662. https://doi.org/10.1007/s00267-012-9961-z

Gashaw, M. (2001). Survival strategies and ecological performances of plants in regularly burnt savannah woodlands and grasslands of western Ethiopia.

Genanaw, A. (2008). Forest Cover Change Detection And Fire Risk Susceptibility Mapping Using GIS And Remote Sensing: Case Of Goba WOREDA. [PhD Thesis]. Addis Ababa University.

Ghobadi, G. J., Gholizadeh, B., & Dashliburun, O. M. (2012). Forest fire risk zone mapping from geographic information system in Northern Forests of Iran (Case study, Golestan province). International Journal of Agriculture and Crop Sciences, 4(12), 818–824.

Ghorbanzadeh, O., Blaschke, T., Gholamnia, K., & Aryal, J. (2019). Forest fire susceptibility and risk mapping using social/infrastructural vulnerability and environmental variables. Fire, 2(3), 50.

Halmy, M. W. A., Gessler, P. E., Hicke, J. A., & Salem, B. B. (2015). Land use/land cover change detection and prediction in the north-western coastal desert of Egypt using Markov-CA. Applied Geography, 63, 101–112. https://doi.org/10.1016/j.apgeog.2015.06.015

Hassen, E. E. (2018). Land Use/Land Cover Dynamics and Driving Forces in Simien Mountains National Park, Amhara Region, Ethiopia. Ethiopian Renaissance Journal of Social Sciences and the Humanities, 5(1), 16–16.

Heo, J., Park, J. S., Song, Y.-S., Lee, S. K., & Sohn, H.-G. (2008). An integrated methodology for estimation of forest fire-loss using geospatial information. Environmental Monitoring and Assessment, 144(1), 285–299.

Kant, S. L., Kanga, S., Singh, N. M., Sinha, S., & Chandra, P. P. (2012). Fuzzy AHP for forest fire risk modeling. Disaster Prevention and Management: An International Journal, 21(2), 160–171. https://doi.org/10.1108/09653561211219964

Lentile*, L. B., Holden*, Z. A., Smith*, A. M. S., Falkowski, M. J., Hudak, A. T., Morgan, P., Lewis, S. A., Gessler, P. E., Benson, N. C., Lentile*, L. B., Holden*, Z. A., Smith*, A. M. S., Falkowski, M. J., Hudak, A. T., Morgan, P., Lewis, S. A., Gessler, P. E., & Benson, N. C. (2006). Remote sensing techniques to assess active fire characteristics and post-fire effects. International Journal of Wildland Fire, 15(3), 319–345. https://doi.org/10.1071/WF05097

Masresha, G. (2019). Study on Temporal Alterations in Land Cover Types in Simien Mountain National Park, Northwest Ethiopia. International Journal of Sustainable Agricultural Research, 6(3), 125–136.

Melchiorre, A., & Boschetti, L. (2018). Global Analysis of Burned Area Persistence Time with MODIS Data. Remote Sensing, 10(5), 750. https://doi.org/10.3390/rs10050750

Monitoring land use/cover change using remote sensing and GIS techniques: A case study of Hawalbagh block, district Almora, Uttarakhand, India. (2015). The Egyptian Journal of Remote Sensing and Space Science, 18(1), 77–84. https://doi.org/10.1016/j.ejrs.2015.02.002

Neubert, M., & Meinel, G. (2005). Atmospheric and terrain correction of IKONOS imagery using ATCOR3. Proc. ISPRS Hanover Workshop.

Orozco, S. J. (2008). Forest fire risk model for Michoacan, Mexico.

Parajuli, A., Gautam, A. P., Sharma, S. P., Bhujel, K. B., Sharma, G., Thapa, P. B., Bist, B. S., & Poudel, S. (2020). Forest fire risk mapping using GIS and remote sensing in two major landscapes of Nepal. Geomatics, Natural Hazards and Risk, 11(1), 2569–2586. https://doi.org/10.1080/19475705.2020.1853251

Polychronaki, A., & Gitas, I. Z. (2012). Burned Area Mapping in Greece Using SPOT-4 HRVIR Images and Object-Based Image Analysis. Remote Sensing, 4(2), 424–438. https://doi.org/10.3390/rs4020424

Ridwan, M. A., Radzi, N. a. M., Ahmad, W. S. H. M. W., Mustafa, I. S., Din, N. M., Jalil, Y. E., Isa, A. M., Othman, N. S., & Zaki, W. M. D. W. (2018). Applications of landsat-8 data: A Survey. https://doi.org/10.14419/ijet.v7i4.35.22858

Rodriguez, M. (2021). A Comprehensive Study of Forest Health and Structure Following the West Fork Fire Complex in Southwest Colorado through Normalized Difference Vegetation

Index (NDVI) and Normalized Burn Ratio (NBR). https://repository.arizona.edu/handle/10150/659898

Roy, D. P., Boschetti, L., & Trigg, S. N. (2006). Remote sensing of fire severity: Assessing the performance of the normalized burn ratio. IEEE Geoscience and Remote Sensing Letters, 3(1), 112–116. https://doi.org/10.1109/LGRS.2005.858485

Roy, P. S. (N.D.). Forest Fire And Degradation Assessment Using Satellite Remote Sensing and Geographic Information System. 40.

Saklani, P. (2008). Forest Fire Risk Zonation: A Case Study Pauri Garhwal, Uttrakhand, India.

Shiferaw, D., & Suryabhagavan, K. V. (2019). Forest degradation monitoring and assessment of biomass in Harenna Buluk District, Bale Zone, Ethiopia: A geospatial perspective. Tropical Ecology, 60(1), 94–104. https://doi.org/10.1007/s42965-019-00012-5

Storey, J., Scaramuzza, P., Schmidt, G., & Barsi, J. (2005). Landsat 7 Scan Line Corrector-Off Gap-Filled Product Development. 13.

Sunar, F., & Özkan, C. (2001). Forest fire analysis with remote sensing data. International Journal of Remote Sensing, 22(12), 2265–2277.

Suryabhagavan, K. V., Alemu, M., & Balakrishnan, M. (2016). GIS-based multi-criteria decision analysis for forest fire susceptibility mapping: A case study in Harenna forest, southwestern Ethiopia. Tropical Ecology, 57(1), 33–43.

Syphard, A. D., Radeloff, V. C., Keeley, J. E., Hawbaker, T. J., Clayton, M. K., Stewart, S. I., & Hammer, R. B. (2007). HUMAN INFLUENCE ON CALIFORNIA FIRE REGIMES. Ecological Applications, 17(5), 1388–1402. https://doi.org/10.1890/06-1128.1

Tafesse, M. (2016). Forest Fire Risk Zone Modeling and Mapping in Bale Mountains National Park (Bmnp), Oromia, Ethiopia [Thesis, Addis Ababa Universty]. http://etd.aau.edu.et/handle/123456789/7148

Tan, Z., Tieszen, L. L., Zhu, Z., Liu, S., & Howard, S. M. (2007). An estimate of carbon emissions from 2004 wildfires across Alaskan Yukon River Basin. Carbon Balance and Management, 2(1), 12. https://doi.org/10.1186/1750-0680-2-12

Tekalign, W., & Kebede, Y. (2016). Impacts of Wildfire and Prescribed Fire on Wildlife and Habitats: A Review. 13.

Teketay, D. (2000, January 1). Vegetation Types and Forest Fire Management in Ethiopia.

Tran, B. N., Tanase, M. A., Bennett, L. T., & Aponte, C. (2018). Evaluation of Spectral Indices for Assessing Fire Severity in Australian Temperate Forests. Remote Sensing, 10(11), 1680. https://doi.org/10.3390/rs10111680

Uncontrolled wildfire burns Ethiopia's Simien Mountains National Park. (2019, April 13). InfoNile. https://www.infonile.org/en/2019/04/uncontrolled-wildfire-burns-ethiopias-simien-mountains-national-park/

Vedovato, L., Jacon, A., Lima, A., Moreira Pessôa, A. C., & Aragão, L. (2015). Detection of burned forests in Amazonia using the Normalized Burn Ratio (NBR) and Linear Spectral Mixture Model from Landsat 8 images.

Veraverbeke, S., Lhermitte, S., Verstraeten, W. W., & Goossens, R. (2010). The temporal dimension of differenced Normalized Burn Ratio (dNBR) fire/burn severity studies: The case of the large 2007 Peloponnese wildfires in Greece. Remote Sensing of Environment, 114(11), 2548–2563. https://doi.org/10.1016/j.rse.2010.05.029

Vermote, E. F., & Kotchenova, S. (2008). Atmospheric correction for the monitoring of land surfaces. Journal of Geophysical Research: Atmospheres, 113(D23). https://doi.org/10.1029/2007JD009662

Viana, C. M., Oliveira, S., Oliveira, S. C., & Rocha, J. (2019). 29—Land Use/Land Cover Change Detection and Urban Sprawl Analysis. In H. R. Pourghasemi & C. Gokceoglu (Eds.), Spatial Modeling in GIS and R for Earth and Environmental Sciences (pp. 621–651). Elsevier. https://doi.org/10.1016/B978-0-12-815226-3.00029-6

Vicente-Serrano, S. M., Quiring, S. M., Peña-Gallardo, M., Yuan, S., & Domínguez-Castro, F. (2020). A review of environmental droughts: Increased risk under global warming? Earth-Science Reviews, 201, 102953. https://doi.org/10.1016/j.earscirev.2019.102953

Wang, W., Ma, X., Moazzam Nizami, S., Tian, C., & Guo, F. (2018). Anthropogenic and Biophysical Factors Associated with Vegetation Restoration in Changting, China. Forests, 9(6), 306. https://doi.org/10.3390/f9060306

Yakubu, I., Mireku-Gyimah, D., & Duker, A. A. (2015). Review of methods for modelling forest fire risk and hazard. African Journal of Environmental Science and Technology, 9(3), 155–165. https://doi.org/10.4314/ajest.v9i3.

Yihune, M., Bekele, A., & Tefera, Z. (2009). Human–gelada baboon conflict in and around the Simien Mountains National Park, Ethiopia. African Journal of Ecology, 47(3), 276–282.

# Appendix

**Appendix 1: Accuracy assessment points for LULC 2010**

| Id | Easting | Northing | LULC class | Id | Easting | Northing | LULC class |
|---|---|---|---|---|---|---|---|
| 1 | 395595 | 1461296 | Shrubs | 41 | 404031 | 1469552 | Shrubs |
| 2 | 395650 | 1461465 | Shrubs | 42 | 404048 | 1469442 | Shrubs |
| 3 | 395775 | 1461410 | Shrubs | 43 | 404115 | 1469164 | Shrubs |
| 4 | 395719 | 1461544 | Shrubs | 44 | 404132 | 1469001 | Shrubs |
| 5 | 395508 | 1461507 | Shrubs | 45 | 404276 | 1468925 | Shrubs |
| 6 | 395330 | 1461505 | Shrubs | 46 | 404473 | 1468805 | Shrubs |
| 7 | 395341 | 1461322 | Shrubs | 47 | 404547 | 1468705 | Shrubs |
| 8 | 395299 | 1461137 | Shrubs | 48 | 404361 | 1468661 | Shrubs |
| 9 | 395346 | 1460970 | Shrubs | 49 | 406160 | 1468119 | Shrubs |
| 10 | 395095 | 1461116 | Shrubs | 51 | 405957 | 1467586 | Grassland |
| 11 | 394873 | 1461121 | Shrubs | 52 | 406179 | 1467776 | Grassland |
| 12 | 394690 | 1461253 | Shrubs | 53 | 406046 | 1467744 | Grassland |
| 13 | 394735 | 1461507 | Shrubs | 54 | 408211 | 1467274 | Grassland |
| 14 | 395341 | 1461748 | Shrubs | 55 | 407811 | 1465998 | Grassland |
| 15 | 394140 | 1461878 | Shrubs | 56 | 407773 | 1466157 | Grassland |
| 16 | 394116 | 1462161 | Shrubs | 57 | 407716 | 1466271 | Grassland |
| 17 | 394714 | 1462119 | Shrubs | 58 | 407786 | 1466519 | Grassland |
| 18 | 394105 | 1462267 | Shrubs | 59 | 404026 | 1467789 | Grassland |
| 19 | 396328 | 1462607 | Shrubs | 60 | 404128 | 1467649 | Grassland |
| 20 | 407293 | 1465802 | Shrubs | 61 | 404230 | 1467541 | Grassland |
| 21 | 406954 | 1465876 | Shrubs | 62 | 404172 | 1467452 | Grassland |
| 22 | 407060 | 1466103 | Shrubs | 63 | 404261 | 1467643 | Grassland |
| 23 | 407256 | 1465976 | Shrubs | 64 | 404166 | 1467782 | Grassland |
| 24 | 407415 | 1466336 | Shrubs | 65 | 404115 | 1467916 | Grassland |
| 25 | 408121 | 1467085 | Shrubs | 66 | 403938 | 1467859 | Grassland |
| 26 | 408170 | 1466914 | Shrubs | 67 | 403785 | 1467865 | Grassland |
| 27 | 408197 | 1466770 | Shrubs | 68 | 403626 | 1467846 | Grassland |
| 28 | 408275 | 1466683 | Shrubs | 69 | 403703 | 1467744 | Grassland |
| 29 | 408195 | 1466544 | Shrubs | 70 | 403474 | 1467852 | Grassland |
| 30 | 404299 | 1468749 | Shrubs | 71 | 403417 | 1467706 | Grassland |
| 31 | 404026 | 1468908 | Shrubs | 72 | 403303 | 1467738 | Grassland |
| 32 | 404147 | 1469264 | Shrubs | 73 | 403207 | 1467674 | Grassland |
| 33 | 404183 | 1469461 | Shrubs | 74 | 403131 | 1467509 | Grassland |
| 34 | 404333 | 1469465 | Shrubs | 75 | 403004 | 1467281 | Grassland |
| 35 | 404564 | 1469473 | Shrubs | 76 | 403169 | 1467211 | Grassland |
| 36 | 404693 | 1469440 | Shrubs | 77 | 403341 | 1467293 | Grassland |
| 37 | 404816 | 1469461 | Shrubs | 78 | 405011 | 1466678 | Grassland |
| 38 | 404687 | 1469562 | Shrubs | 79 | 404833 | 1466830 | Grassland |
| 39 | 404496 | 1469545 | Shrubs | 80 | 404954 | 1466843 | Grassland |
| 40 | 404194 | 1469562 | Shrubs | 81 | 405030 | 1466951 | Grassland |

| | | | | | | | |
|---|---|---|---|---|---|---|---|
| 82 | 405119 | 1467008 | Grassland | 127 | 405751 | 1466030 | Forest |
| 83 | 405785 | 1467376 | Grassland | 128 | 405968 | 1466046 | Forest |
| 84 | 407576 | 1466970 | Grassland | 129 | 406151 | 1466080 | Forest |
| 85 | 407690 | 1467065 | Grassland | 130 | 405942 | 1466184 | Forest |
| 86 | 407811 | 1467090 | Grassland | 131 | 405804 | 1466260 | Forest |
| 87 | 404255 | 1468299 | Grassland | 132 | 405714 | 1466154 | Forest |
| 88 | 404313 | 1468444 | Grassland | 133 | 405555 | 1466154 | Forest |
| 89 | 404374 | 1468320 | Grassland | 134 | 405325 | 1466030 | Forest |
| 90 | 404080 | 1468349 | Grassland | 135 | 405455 | 1465840 | Forest |
| 91 | 404152 | 1468436 | Grassland | 136 | 405500 | 1465694 | Forest |
| 92 | 404178 | 1468328 | Grassland | 137 | 405383 | 1465641 | Forest |
| 93 | 404173 | 1468243 | Grassland | 138 | 405394 | 1465538 | Forest |
| 94 | 403975 | 1468225 | Grassland | 139 | 405486 | 1465620 | Forest |
| 95 | 404538 | 1468389 | Grassland | 140 | 405613 | 1465800 | Forest |
| 96 | 396333 | 1461645 | Forest | 141 | 405664 | 1465914 | Forest |
| 97 | 396519 | 1461693 | Forest | 127 | 405751 | 1466030 | Forest |
| 98 | 396650 | 1461713 | Forest | 128 | 405968 | 1466046 | Forest |
| 99 | 396063 | 1461733 | Forest | 129 | 406151 | 1466080 | Forest |
| 100 | 395829 | 1461820 | Forest | 130 | 405942 | 1466184 | Forest |
| 101 | 395928 | 1461876 | Forest | 131 | 405804 | 1466260 | Forest |
| 102 | 395714 | 1461991 | Forest | 132 | 405714 | 1466154 | Forest |
| 103 | 395686 | 1461784 | Forest | 133 | 405555 | 1466154 | Forest |
| 104 | 395634 | 1461967 | Forest | 134 | 405325 | 1466030 | Forest |
| 105 | 395590 | 1462034 | Forest | 135 | 405455 | 1465840 | Forest |
| 106 | 395991 | 1462074 | Forest | 136 | 405500 | 1465694 | Forest |
| 107 | 396591 | 1462106 | Forest | 137 | 405383 | 1465641 | Forest |
| 108 | 396424 | 1462042 | Forest | 138 | 405394 | 1465538 | Forest |
| 109 | 396698 | 1462193 | Forest | 139 | 405486 | 1465620 | Forest |
| 110 | 396805 | 1462106 | Forest | 140 | 405613 | 1465800 | Forest |
| 111 | 396785 | 1461947 | Forest | 141 | 405664 | 1465914 | Forest |
| 112 | 396122 | 1461229 | Forest | 142 | 405793 | 1465940 | Forest |
| 113 | 396043 | 1461320 | Forest | 143 | 405934 | 1465956 | Forest |
| 114 | 396948 | 1462134 | Forest | 144 | 406039 | 1465980 | Forest |
| 115 | 396880 | 1462245 | Forest | 145 | 406455 | 1465967 | Forest |
| 116 | 391357 | 1461660 | Forest | 146 | 406852 | 1466390 | Forest |
| 117 | 391152 | 1461680 | Forest | 147 | 406878 | 1466784 | Forest |
| 118 | 390801 | 1461878 | Forest | 148 | 402446 | 1463044 | Forest |
| 119 | 390907 | 1462064 | Forest | 149 | 403002 | 1463774 | Farmland |
| 120 | 390933 | 1461587 | Forest | 150 | 403240 | 1463806 | Farmland |
| 121 | 390748 | 1461422 | Forest | 151 | 402859 | 1463488 | Farmland |
| 122 | 390748 | 1461078 | Forest | 152 | 402446 | 1463679 | Farmland |
| 123 | 390867 | 1460767 | Forest | 153 | 402843 | 1464139 | Farmland |
| 124 | 390550 | 1460284 | Forest | 154 | 403447 | 1464647 | Farmland |
| 125 | 389908 | 1461190 | Forest | 155 | 403701 | 1464282 | Farmland |
| 126 | 405531 | 1465959 | Forest | 156 | 403415 | 1464235 | Farmland |
| | | | | | | | |

| 157 | 403605 | 1463949 | Farmland | 203 | 425951 | 1471559 | Bare Land |
|---|---|---|---|---|---|---|---|
| 158 | 403478 | 1463488 | Farmland | 204 | 425427 | 1471623 | Bare Land |
| 159 | 403129 | 1463250 | Farmland | 205 | 427714 | 1469781 | Bare Land |
| 160 | 402605 | 1463171 | Farmland | 206 | 427523 | 1470051 | Bare Land |
| 161 | 401827 | 1463298 | Farmland | 207 | 427317 | 1470258 | Bare Land |
| 162 | 401621 | 1463790 | Farmland | 208 | 427063 | 1470480 | Bare Land |
| 163 | 401764 | 1464076 | Farmland | 209 | 431468 | 1463222 | Bare Land |
| 164 | 402097 | 1464266 | Farmland | 210 | 431812 | 1463130 | Bare Land |
| 165 | 402129 | 1464504 | Farmland | 211 | 431719 | 1463394 | Bare Land |
| 166 | 402970 | 1464933 | Farmland | 212 | 431878 | 1463474 | Bare Land |
| 167 | 403478 | 1464965 | Farmland | 213 | 431110 | 1462826 | Bare Land |
| 168 | 401351 | 1465092 | Farmland | 214 | 430886 | 1462693 | Bare Land |
| 169 | 401684 | 1465362 | Farmland | 215 | 430542 | 1462759 | Bare Land |
| 170 | 402081 | 1465743 | Farmland | 216 | 430370 | 1462799 | Bare Land |
| 171 | 402161 | 1465266 | Farmland | 217 | 432671 | 1465352 | Bare Land |
| 172 | 401891 | 1464949 | Farmland | 218 | 432513 | 1465485 | Bare Land |
| 173 | 401399 | 1464743 | Farmland | 219 | 414940 | 1463857 | Bare Land |
| 174 | 401557 | 1465028 | Farmland | 220 | 415363 | 1463950 | Bare Land |
| 175 | 401335 | 1465552 | Farmland | 221 | 415859 | 1461829 | Bare Land |
| 176 | 401907 | 1465568 | Farmland | 222 | 415978 | 1461890 | Bare Land |
| 177 | 402002 | 1466044 | Farmland | 223 | 416031 | 1462054 | Bare Land |
| 178 | 401161 | 1463473 | Farmland | 224 | 416277 | 1462464 | Bare Land |
| 179 | 401335 | 1464139 | Farmland | 225 | 416250 | 1462564 | Bare Land |
| 180 | 402637 | 1465886 | Farmland | 226 | 415727 | 1461363 | Bare Land |
| 181 | 401084 | 1465609 | Farmland | 227 | 415777 | 1461429 | Bare Land |
| 182 | 418415 | 1470049 | Farmland | 228 | 415901 | 1461474 | Bare Land |
| 183 | 418605 | 1469462 | Farmland | 229 | 415774 | 1461599 | Bare Land |
| 184 | 418616 | 1469610 | Farmland | 230 | 422229 | 1475215 | Bare Land |
| 185 | 418542 | 1469752 | Farmland | 231 | 422300 | 1475373 | Bare Land |
| 186 | 418517 | 1469889 | Farmland | 232 | 422451 | 1475500 | Bare Land |
| 187 | 418466 | 1469737 | Farmland | 233 | 422729 | 1475532 | Bare Land |
| 188 | 418663 | 1469698 | Farmland | 234 | 420554 | 1474746 | Bare Land |
| 189 | 418571 | 1469827 | Farmland | 235 | 420149 | 1474635 | Bare Land |
| 190 | 418499 | 1469842 | Farmland | 236 | 420117 | 1474310 | Bare Land |
| 191 | 418419 | 1469897 | Farmland | 237 | 419975 | 1474064 | Bare Land |
| 192 | 418424 | 1469971 | Farmland | 238 | 422335 | 1477165 | Bare Land |
| 193 | 418525 | 1469977 | Farmland | 239 | 422409 | 1477350 | Bare Land |
| 194 | 418222 | 1470226 | Farmland | 240 | 422594 | 1477482 | Bare Land |
| 195 | 418183 | 1470081 | Farmland | 241 | 422726 | 1477556 | Bare Land |
| 196 | 418361 | 1470445 | Farmland | 242 | 423165 | 1477842 | Bare Land |
| 197 | 418242 | 1469988 | Farmland | 243 | 423065 | 1477784 | Bare Land |
| 198 | 418441 | 1470279 | Farmland | 244 | 423308 | 1477942 | Bare Land |
| 199 | 427142 | 1470654 | bare land | 245 | 423531 | 1477948 | Bare Land |
| 200 | 426809 | 1470924 | bare land | 246 | 423853 | 1478218 | Bare Land |
| 201 | 426634 | 1471274 | bare land | 247 | 422308 | 1476990 | Bare Land |
| 202 | 426285 | 1471416 | bare land | 248 | 422684 | 1475672 | Bare Land |

**Appendix 2: validation points of the forest fire risk model**

| ID | Easting | Northing | FIT_ON | ID | Easting | Northing | FIT_ON |
|---|---|---|---|---|---|---|---|
| 1 | 421813 | 1475789 | High | 37 | 420070 | 1476045 | High |
| 2 | 420258 | 1477105 | High | 38 | 420568 | 1473443 | High |
| 3 | 420093 | 1475345 | High | 39 | 421906 | 1477146 | High |
| 4 | 421162 | 1477057 | Very High | 40 | 421634 | 1474499 | Very High |
| 5 | 423325 | 1477348 | High | 41 | 421728 | 1474030 | High |
| 6 | 422575 | 1476752 | Moderate | 42 | 420937 | 1473508 | High |
| 7 | 422346 | 1477879 | High | 43 | 423318 | 1476532 | High |
| 8 | 419916 | 1475836 | High | 44 | 422027 | 1476135 | Very High |
| 9 | 421669 | 1476138 | High | 45 | 421452 | 1473702 | High |
| 10 | 422335 | 1476217 | High | 46 | 420460 | 1473733 | High |
| 11 | 421536 | 1475474 | Very High | 47 | 421415 | 1473991 | High |
| 12 | 420927 | 1475210 | High | 48 | 423089 | 1476413 | Very High |
| 13 | 420641 | 1476268 | Very High | 49 | 421659 | 1476504 | Very High |
| 14 | 420892 | 1476491 | Very High | 50 | 420928 | 1474071 | High |
| 15 | 419581 | 1474953 | Moderate | 51 | 421615 | 1477100 | Very High |
| 16 | 419661 | 1475484 | High | 52 | 421854 | 1476719 | Very High |
| 17 | 421324 | 1476256 | High | 53 | 422845 | 1474778 | High |
| 18 | 420453 | 1475971 | High | 54 | 421619 | 1476793 | Very High |
| 19 | 421195 | 1475401 | Very High | 55 | 422894 | 1476621 | Very High |
| 20 | 419853 | 1475241 | High | 56 | 421227 | 1476642 | High |
| 21 | 421760 | 1475153 | Very High | 57 | 421000 | 1473842 | High |
| 22 | 422170 | 1474030 | High | 58 | 422050 | 1476472 | Very High |
| 23 | 421037 | 1475463 | Very High | 59 | 422183 | 1477608 | High |
| 24 | 420664 | 1475511 | Very High | 60 | 422256 | 1478080 | High |
| 25 | 423837 | 1476547 | High | 61 | 422110 | 1476701 | Very High |
| 26 | 421650 | 1474746 | Very High | 62 | 422107 | 1474431 | Moderate |
| 27 | 421451 | 1475186 | Very High | 63 | 421000 | 1474498 | Moderate |
| 28 | 420860 | 1475404 | Very High | 64 | 421224 | 1474695 | Moderate |
| 29 | 420995 | 1474299 | High | 65 | 420979 | 1475985 | Very High |
| 30 | 421393 | 1475913 | Very High | 66 | 421648 | 1475261 | Very High |
| 31 | 421217 | 1475065 | High | 67 | 420938 | 1474971 | High |
| 32 | 420116 | 1475718 | High | 68 | 420001 | 1476218 | High |
| 33 | 421647 | 1475619 | Very High | 69 | 420791 | 1475989 | Very High |
| 34 | 420187 | 1473339 | High | 70 | 420525 | 1475709 | Moderate |
| 35 | 421209 | 1475768 | Very High | 71 | 419912 | 1475572 | High |
| 36 | 420328 | 1475790 | High | 72 | 419598 | 1475693 | High |
| | | | | | | | |
| | | | | | | | |

| | | | | | | | |
|---|---|---|---|---|---|---|---|
| 73 | 420741 | 1475693 | Very High | 113 | 420423 | 1476742 | Very High |
| 74 | 421250 | 1475261 | High | 114 | 422790 | 1477138 | Moderate |
| 75 | 422386 | 1473794 | High | 115 | 422183 | 1475529 | Very High |
| 76 | 420310 | 1475352 | High | 116 | 420992 | 1476768 | Very High |
| 77 | 421295 | 1475603 | Very High | 117 | 423536 | 1476030 | High |
| 78 | 421433 | 1474951 | Very High | 118 | 423629 | 1475717 | High |
| 79 | 421931 | 1475259 | Very High | 119 | 423316 | 1475885 | High |
| 80 | 423353 | 1475639 | High | 120 | 422154 | 1475359 | Very High |
| 81 | 421104 | 1476387 | Very High | 121 | 422238 | 1475187 | Low |
| 82 | 422856 | 1475149 | Very High | 122 | 421942 | 1474886 | Moderate |
| 83 | 422401 | 1476420 | Very High | 123 | 421902 | 1475556 | High |
| 84 | 423592 | 1476449 | High | 124 | 422843 | 1476170 | High |
| 85 | 422591 | 1476186 | High | 125 | 422370 | 1475946 | High |
| 86 | 423105 | 1476191 | High | 126 | 422665 | 1476447 | High |
| 87 | 420961 | 1476195 | Very High | 127 | 422853 | 1475696 | High |
| 88 | 420427 | 1476458 | Very High | 128 | 422178 | 1475827 | Very High |
| 89 | 419650 | 1475912 | High | 129 | 422625 | 1475919 | High |
| 90 | 420737 | 1474588 | Low | | | | |
| 91 | 420719 | 1474759 | Low | | | | |
| 92 | 420528 | 1475173 | Low | | | | |
| 93 | 420987 | 1474756 | Low | | | | |
| 94 | 419076 | 1476237 | Moderate | | | | |
| 95 | 422349 | 1476967 | Moderate | | | | |
| 96 | 420399 | 1474468 | Low | | | | |
| 97 | 421185 | 1474893 | High | | | | |
| 98 | 420080 | 1474756 | High | | | | |
| 99 | 419903 | 1477008 | High | | | | |
| 100 | 420358 | 1474676 | High | | | | |
| 101 | 420061 | 1476383 | Very High | | | | |
| 102 | 419498 | 1476401 | Moderate | | | | |
| 103 | 420223 | 1475530 | High | | | | |
| 104 | 420076 | 1477270 | High | | | | |
| 105 | 419860 | 1476772 | High | | | | |
| 106 | 422419 | 1477376 | High | | | | |
| 107 | 419592 | 1476858 | Moderate | | | | |
| 108 | 419895 | 1475011 | Moderate | | | | |
| 109 | 420679 | 1477042 | Very High | | | | |
| 110 | 420233 | 1475169 | High | | | | |
| 111 | 420572 | 1474760 | High | | | | |
| 112 | 419292 | 1475187 | Moderate | | | | |

**Appendix 3: The final result of forest fire risk model of simen mountain national park**

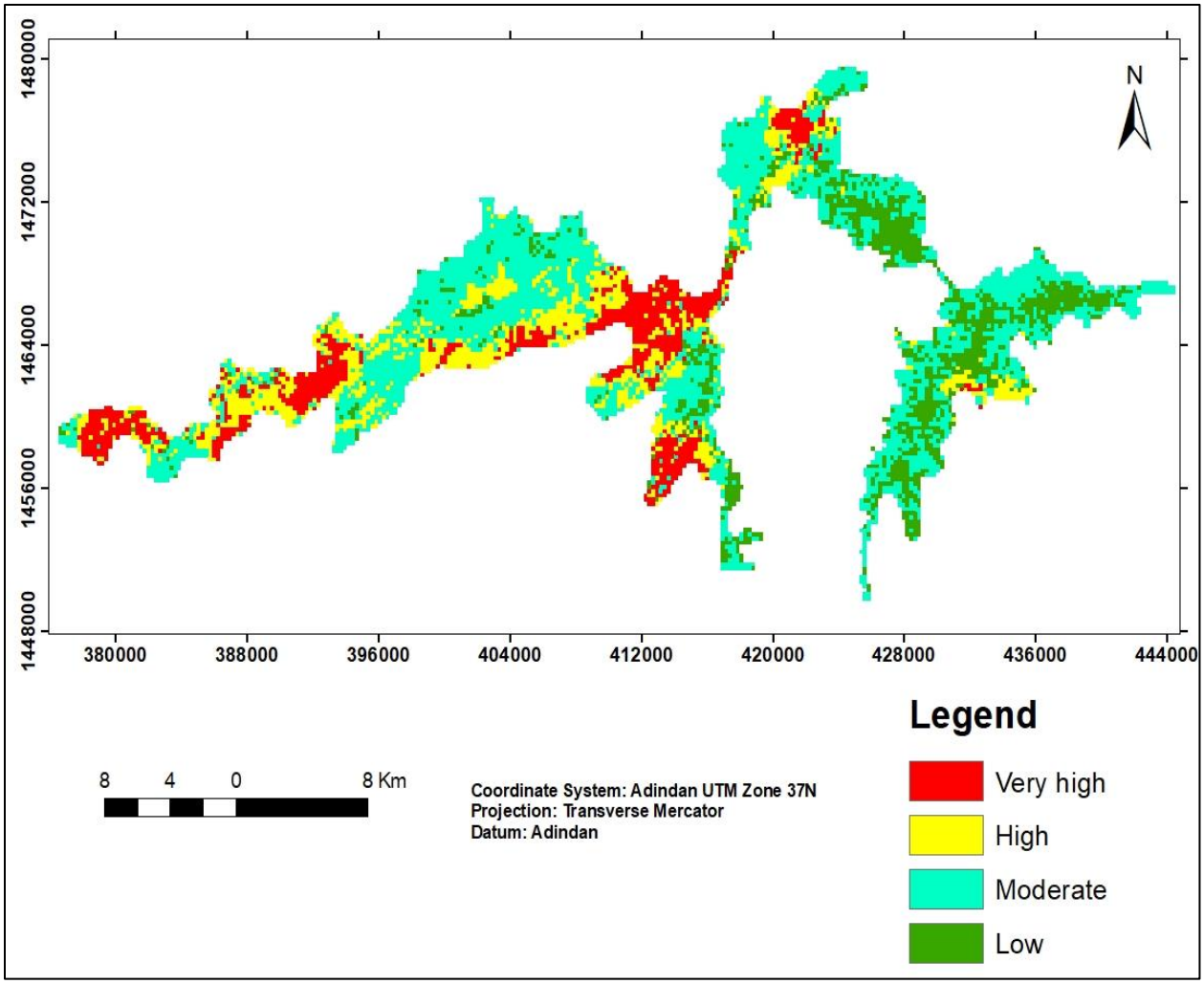

**Appendix 4: Google Earth images pre and post fire of similar area (model validation points were taken on post fire image). The image shows the different between before and after fire.**

**Appendix 5: The following figure shows the validation points taken on the burned areas in the Google Earth image.**

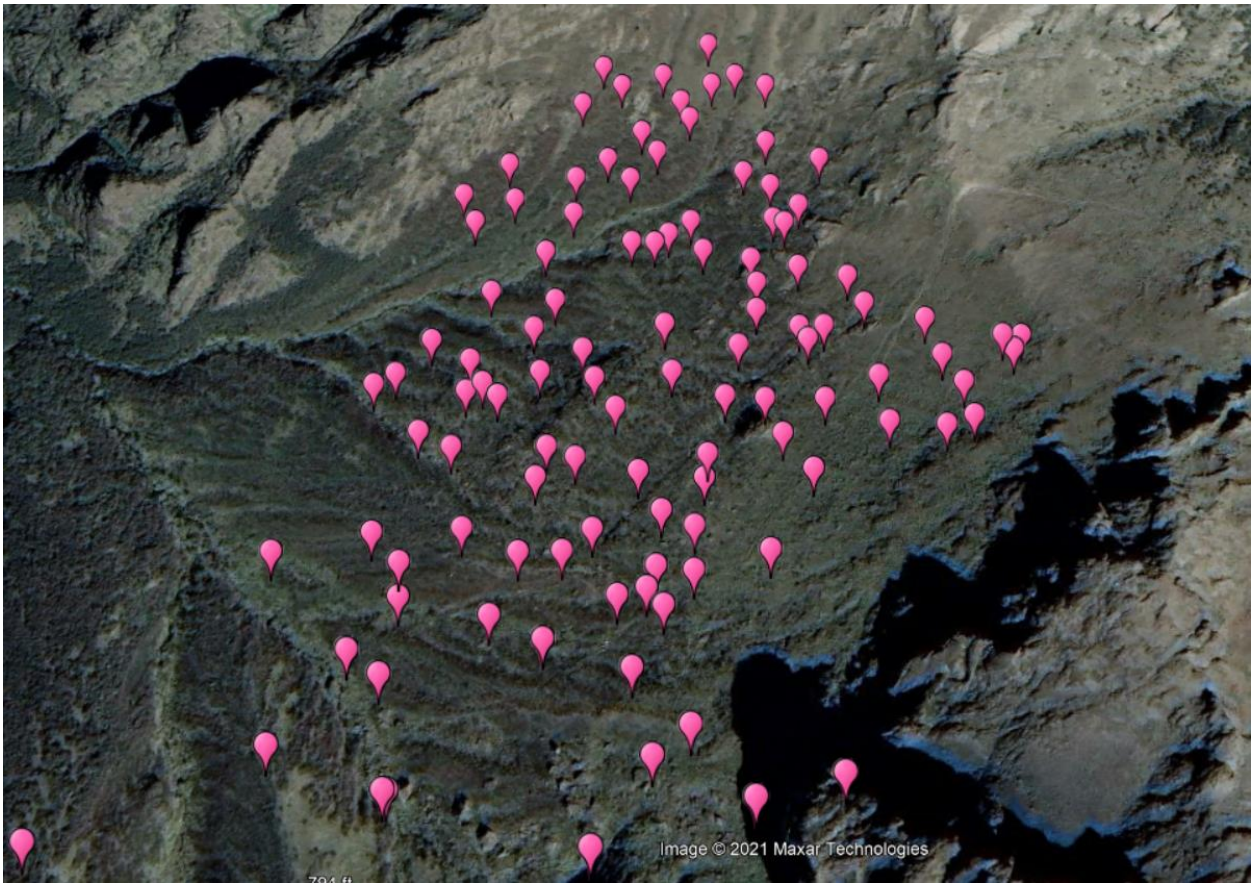

**Appendix 6: Uncontrolled wildfire burns Ethiopia's Simien Mountains National Park (**Source **:***Info Nile*. https://www.infonile.org/en/2019/04/uncontrolled-wildfire-burns-ethiopias-simien-mountains-national-park/**).**


**The above figures (A and B) show during and after burnt areas in SMNP respectively**